C29

Nocodazole disruption of microtubules in the heart of the streptozotocin diabetic rat increases $[Ca^{2+}]_i$ and contraction

H.A. Shiels[2], A.D. O'Connell[1], M.A. Qureshi[3], F.C. Howarth[3], E. White[1] and S.C. Calaghan[1]

[1]School of Biomedical Sciences, University of Leeds, Leeds, UK, [2]School of Biological Sciences, University of Manchester, Manchester, UK and [3]Department of Physiology, United Arab Emirates University, Al Ain, United Arab Emirates

Microtubules in the diabetic heart are resistant to the depolymerising agent colchicine (Howarth *et al.* 2002). Here we examine the functional relevance of these colchicine-stable microtubules, using a high concentration of nocodazole (NOC) which disrupts stable microtubule populations (Webster & Patrick, 2000).

Type 1 diabetes was induced by injection of streptozotocin (STZ; 60 mg kg^{-1} i.p.) in male Wistar rats. 8-12 weeks later, animals were killed humanely, and ventricular myocytes isolated by enzymatic digestion. Myocytes were incubated with vehicle (0.2% DMSO) or 33 μM NOC for 1-3 h. The impact of NOC on microtubule density was assessed in fixed myocytes labelled with an antibody to β-tubulin. The effect of NOC on shortening and the $[Ca^{2+}]_i$ transient (using fura-2) was studied at 36°C (1 Hz stimulation). Statistical analysis was performed using the Student's t test or the χ^2 test.

Microtubule density was 10% higher in myocytes from STZ rats ($P<0.05$) compared with controls. Myocytes from STZ rats showed a tendency for shortening and $[Ca^{2+}]_i$ transient amplitude to be reduced ($P>0.05$). Time to peak $[Ca^{2+}]_i$ was increased ($P<0.05$).

NOC decreased microtubule density in both populations of myocytes, but the effect was greater ($P<0.01$; χ^2 test) in control cells (mean density reduced by 30.7%; n=38-47) than in cells from diabetic rats (mean density reduced by 13.4%, n=56-54). Although the degree of microtubule disruption by NOC was less in myocytes from diabetic rats than controls, the functional consequences of microtubule disruption were much greater. In the presence of NOC, shortening increased by 45.0% in myocytes from STZ rats compared with 4.4% in controls ($P<0.001$; n=18-22; χ^2 test). Likewise, the amplitude of the $[Ca^{2+}]_i$ transient increased by 24.3% in myocytes from STZ rats compared with 6.0% in controls ($P<0.001$, n=19-21; χ^2 test). The prolonged time to peak $[Ca^{2+}]_i$ was absent in myocytes from diabetic animals after treatment with NOC.

Microtubule disruption by NOC has a marked positive inotropic effect in myocytes from diabetic animals which is not seen in controls. This suggests that changes in the cardiac microtubule cytoskeleton are functionally relevant in the STZ model of diabetes. However, a distinction can be drawn between microtubules in STZ-treated animals, which are reported to be hypotensive, and those with hypertension-induced hypertrophy (Tsutsui et al. 1994) where microtubule disruption modifies shortening in the absence of changes in $[Ca^{2+}]_i$.

Howarth FC *et al.* (2002). *Pflugers Archiv* **444**, 432-437.

Tsutsui H *et al.* (1994). *Circ* **90**, 533-555.

Webster DR & Patrick DL (2000). *Am J Physiol* **278**, H1653-H1661.

Supported by the BHF and the British Council.

Where applicable, the experiments described here conform with Physiological Society ethical requirements.

C30

Acute exposure to iron (II) alters Ca^{2+} handling in isolated rat ventricular myocytes

D.T. Baptista-Hon[2], A.C. Elliott[1] and M.E. Diaz[2]

[1]Univ of Manchester, Manchester, UK and [2]Veterinary Biomedical Sciences, Edinburgh University, Edinburgh, UK

Cardiomyopathy and arrhythmias are major causes of mortality in iron poisoning and chronic iron overload (Cohen et al. 2004). However, direct evidence on how toxic concentrations of iron modify cardiac cellular function is scarce. We have examined the acute effects of a large dose of iron (as Fe^{2+}) on Ca^{2+} handling in isolated rat ventricular myocytes.

Rats were humanely killed. Single cardiac ventricular myocytes were isolated by collagenase/protease digestion and loaded with the Ca^{2+}-sensitive fluorescent dye fluo-3. Cells were field-stimulated at 0.33 Hz and cell shortening and Ca^{2+} transients were recorded. Prolonged exposure (30 min) of cells to 500 μM iron (II) (added as iron (III) chloride in the presence of 1 mM of the reducing agent ascorbate) led to a pronounced increase in both the systolic Ca^{2+} transient amplitude and cell shortening (Fig. 1). This was followed after a few minutes (16 ± 8 min, mean ± S.E.M., n = 10) by the appearance of spontaneous Ca^{2+} waves (and propagating waves of contraction), which increased in frequency leading to cell contracture and death. Preloading the cells with the iron chelator deferiprone (DFP; 100 μM) attenuated, but did not completely prevent, the effects of iron (mean time to onset of spontaneous activity in DFP 21 ± 6 min, n = 7, n.s. vs. iron, $p>0.3$ by t test; frequency of spontaneous contractions 6.5 ± 1.4 min^{-1} in iron, 3.1 ± 2.4 min^{-1} with DFP, significantly different with $p<0.03$). In non-stimulated (quiescent) cells, iron treatment led, again after a delay, to the onset of spontaneous contractile activity.

Our results show that iron (II) has acute effects on ventricular cell Ca^{2+} handling that could be arryhthmogenic. The mechanism of these effects is unknown but may be related to the action of oxidative radicals on Ca^{2+} transport processes at the sarcoplasmic reticulum or the sarcolemma.

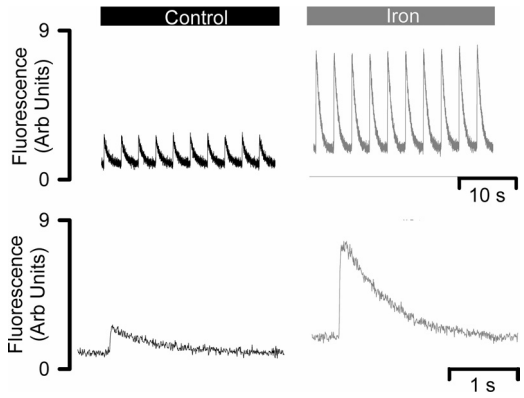

Figure 1. Effects of acute iron exposure on the systolic Ca transient. Original data show: top systolic Ca transients in response to electrical stimulation every 0.33 Hz in control (left) and iron (right). Bottom, average systolic Ca transients taken from the data shown above in control (left) and in iron (right).

Cohen AR, Galanello R, Pennell DJ, Cunningham MJ, Vichinsky E (2004). Thalassemia. Hematology (Am Soc Hematol Educ Program) 14-34.

This work was supported by the British Heart Foundation.

Where applicable, the experiments described here conform with Physiological Society ethical requirements.

C31

Increased susceptibility to pore-opening in heart mitochondria from neonatal compared with adult rats

D. Balaska, A. Halestrap, S. Suleiman and E. Griffiths

Bristol Heart Institute, Department of Biochemistry, University of Bristol, Bristol, UK

The Ca^{2+}-induced mitochondrial permeability transition pore (MPTP) plays a key role in the development of irreversible injury upon reperfusion of hearts following ischaemia. The MPTP can be inhibited in both isolated mitochondria and whole hearts by cyclosporin A (CsA), and this drug can protect adult hearts from reperfusion-induced damage. However, metabolism and mitochodrial function are very different in neonatal hearts, and the susceptibility of these heats to the MPTP has not been studied. Male Wistar rats were humanely killed, and mitochondria isolated from hearts of neonatal (2-3 day old), 7, 14, 21 day old, and adult (2-3 month old) animals. Pore-opening in response to Ca^{2+} was determined spectrophotometrically by monitoring the decrease in absorbance at 520 nm ('swelling'). Mitochondria were incubated overnight for 12-18 h on ice prior to the assay ('aged') to ensure greater consistency because, during the first few hours after isolation, adenine nucleotides may change rapidly which will affect pore opening. ATP and ADP levels were measured in mitochondria from all ages, both in freshly isolated and aged mitochondria. This was achieved with the use of firefly luciferase and measured on a scintillation counter. n = at least 6 separate preparations of mitochondria. Data were analysed by 2-way ANOVA to determine statistical significances.

Table 1 shows that the rates of pore-opening increased with decreasing age at both 10 μM Ca^{2+} ($p<0.001$) and 50 μM Ca^{2+} ($p<0.001$). In addition, whereas CsA almost abolished pore-opening in the adults at [Ca^{2+}] up to 100 μM, in the neonate CsA was only inhibitory up to 10 μM Ca^{2+}.

Further investigation into the mitochondrial content of the ADP and ATP was carried out and it was found that both nucleotide levels were significantly lower in the neonatal mitochondria and increased with age. This confirms the increased pore opening of these mitochondria, even in the presence of CsA, as both ATP and ADP are known to inhibit MPTP opening (1). Thus, neonatal hearts may be much more susceptible to the damage caused by the MPTP upon reperfusion, which will need to be taken into account when designing cardioprotective strategies.

Table 1. Rate of pore opening (ΔA_{520} 10^4 s^{-1}

Age	10μM Ca^{2+} (n=3)	50μM Ca^{2+} (n=6)	80μM Ca^{2+} + 500nM CsA (n=3)
Neonate	0.19 ± 0.01	0.565 ± 0.100	0.417 ± 0.017
7 days	0.105 ± 0.005	0.393 ± 0.065	0.283 ± 0.009
14 days	0.035 ± 0.015	0.221 ± 0.027	0.205 ± 0.045
21 days	0.01 ± 0.001	0.164 ± 0.018	0.048 ± 0.026
Adult	0.015 ± 0.005	0.177 ± 0.021	0.07 ± 0.026

Suleiman M-S, Halestrap AP & Griffiths EJ (2001). Pharmacol Ther 89, 29-46.

This work was supported by the British Heart Foundation.

Where applicable, the experiments described here conform with Physiological Society ethical requirements.

C32

A comparison of electromechanical changes to guinea-pig myocardium in two models of left ventricular hypertrophy

R. Gray[1], M. Turner[2], D. Sheridan[2] and C.H. Fry[1]

[1]Institute of Urology, University College London, London, UK and [2]Academic Cardiology Unit, Imperial College London, London, UK

The aim was to investigate the potential role of the renin-angiotensin system in the electromechanical changes associated with left ventricular hypertrophy (LVH) induced by thoracic aortic constriction, and its regression.

LVH was induced by placing a plastic clip (2mm diameter) around the ascending aorta under anaesthesia (30 mg/kg methohexitone sodium, followed by inhalation of a 49%/49%/2%, N_2O/O_2/halothane mixture). After 42±3 days, animals underwent a second thoracotomy, with an identical anaesthetic procedure, and the plastic clip was either removed (regressed group) or left in place (age-matched LVH group). Following the second operation animals were fed losartan (10 mg/kg/day) or placebo in the drinking water for 42±3 days. Sham-operated and unoperated animals were controls. In another group, angiotensin II (200 ng/kg/min) or saline was infused by subcutaneous osmotic mini-pumps for 42±3 days. After humane killing, the heart was removed, heart-to-body weight ratio (HBR) recorded, and papillary muscles superfused in Tyrode solution at 37°C. Isometric tension and action potential (AP) characteristics were recorded as previously described (Botchway et al. 2004). The force-frequency relationship was quantified as the ratio of peak tensions generated at stimulation frequencies of 1.6 and 0.8 Hz ($T_{1.6/0.8}$). Results are given as mean±SD and statistical significance from control ($p<0.05$) assessed using Student's t tests.

Compared with sham and unoperated animals (n =16), significant changes to the LVH group (n=11) were: an increased HBR; (3.89±0.41 vs 2.75±0.41 g/kg); a decline in the force-frequency response ($T_{1.6/0.8}$) 1.33±0.14 vs 1.52±0.09); a reduction of longitudinal conduction velocity (58.9±3.8 vs 70.9±3.4 cm/s); an increase of transverse conduction velocity (24.2±4.6 vs 19.4±2.7cm/s); and prolongation of the action potential duration (APD) at 1Hz (221.7±14.9 vs 209.4±11.7 ms). With removal of the constriction (n=10) HBR and conduction velocity decreased towards control values (3.15±0.39 g/kg, $p<0.05$ and 66.7±4.7 cm/s, $p<0.05$ respectively) and $T_{1.6/0.8}$ recovered completely (1.52±0.17. Losartan had no effect on these variables in either the LVH or regressed animals. Angiotensin II infusion (n=7) was also accompanied by an increase of HBR (3.57±0.44 vs 2.66±0.24 g/kg), a decline of $T_{1.6/0.8}$ (1.23±0.04 vs 1.55±0.05), but no change to longitudinal conduction velocity (72.2±4.1 vs 73.2±2.1 cm/s) or APD (206.4±17.9 vs 209.4±11.7ms) compared to saline infusion (n=6). Transverse conduction velocity increased from 17.5±1.8 to 23.2±3.9 cm/s).

We conclude that electromechanical changes to hypertrophied myocardium are different in these two models of LVH. Furthermore, angiotensin II receptor blockade has no effect on the electromechanical changes induced by thoracic aortic constriction.

Botchway et al. (2004). Cardiovasc Res 60, 510-517.

We thank the British Heart Foundation for financial assistance.

Where applicable, the experiments described here conform with Physiological Society ethical requirements.

C33

Effect of voluntary exercise on the regional variation in transient outward potassium current density, I_{to}, and the expression of its encoding mRNAs, in isolated rat ventricular myocytes

R. Stones, R. Billeter, S. Harrison and E. White

Biomedical Sciences, The University of Leeds, Leeds, UK

We have previously reported a lengthening of the action potential of single rat sub-epicardial left ventricular myocytes (EPI) isolated from the hearts of female animals that undertook 6-7 weeks of voluntary wheel running (Natali *et al.* 2002). We have tested the hypothesis that a decrease in the transient outward current (Ito) might contribute to this change in action potential configuration.

Ito was measured under whole cell, voltage clamp conditions at 37°C in single EPI and sub-endocardial myocytes (ENDO) isolated from hearts of humanely killed female Sprague-Dawley rats undergoing 6-7 weeks of voluntary wheel running (TRN) or their sedentary equivalents (SED). Tissue samples from these four groups were also analysed using real-time reverse transcription polymerase chain reaction to measure the mRNA expression ratios of Kv4.2, Kv4.3 and Kv1.4, genes which encode for cardiac Ito. For each transcript, 3 measurements were performed on every cDNA sample and ratios relative to 6 of the cDNA samples, which were selected as reference standards, were determined from the respective delta CT (crossing point) value and average efficiency of the reaction. These ratios were then related to the average content of 28S cDNA in each sample.

Ito density was dependent upon region being significantly greater in EPI than ENDO for both SED and TRN (Ito recorded between -40 and +60mV, $P<0.05$, two way repeated measures ANOVA, n = 13-28 cells in each group). However, whilst there was no significant difference in the density of Ito in ENDO between TRN and SED, there was a statistically significant decrease in Ito recorded between -40 and +60mV in TRN EPI compared with SED EPI ($P<0.05$, two-way repeated measures ANOVA, n = 13-28 cells in each group). In addition, normalised Ito density recorded in individual TRN EPI myocytes at +40mV was found to be inversely proportional to cell size (linear regression, R=-0.529, $P<0.05$ Spearman Rank order correlation, n=28). Kv4.2 expression was similarly dependent upon region (EPI > ENDO) but in addition was increased by voluntary exercise (3.87±0.29 vs 3.03±0.22 mRNA expression ratios in TRN EPI vs SED EPI respectively, (mean ± S.E.M.) $P< 0.05$, 2 way ANOVA, n=10 in each group). This may be a response to the functional decrease in Ito. Expression of Kv4.3 and Kv1.4 did not correlate with changes in Ito density.

We conclude that a regionally dependent decrease in Ito current may explain the effect of voluntary exercise on the action potential configuration of single rat ventricular myocytes.

Natali AJ *et al.* (2002). *J Physiol* **541**, 863-875.

This work was funded by the British Heart Foundation.

Where applicable, the experiments described here conform with Physiological Society ethical requirements.

C34

Isolated working hypertrophic but not normotrophic rat heart is protected by glutamate during ischaemia and reperfusion

N. King, H. Lin and M. Suleiman

Clinical Science at South Bristol, University of Bristol, Bristol, UK

Metabolic differences have been reported between normal and hypertrophic hearts (Suleiman *et al.* 1998). Moreover, the expression and activity of the glutamate transporters, EAAT1 and 3 are significantly increased in hypertrophic compared to control heart (King *et al.* 2004a, b). This suggests that lower concentrations of glutamate will be needed to protect the hypertrophic myocardium against ischaemia and reperfusion injury. Therefore, the effect of supplementation with 0.5mM glutamate during ischaemia and reperfusion was investigated using isolated and perfused hypertrophic hearts from spontaneously hypertensive rats (SHR) and their corresponding control hearts from normotensive Wistar Kyoto (WKY) rats.

Male SHR and WKY rats were humanely killed and the hearts dissected. Isolated working rat hearts were perfused with Krebs buffer at 37°C as described previously (Javadov *et al.* 2000). After 25 min equilibration in the working mode, hearts were exposed to normothermic global ischaemia for 20 min. Hearts were then reperfused and functional recovery and release of lactate dehydrogenase (LDH) determined. Where used, 0.5mM glutamate was present before and during ischaemia, but was washed out after 10 min reperfusion. Data are expressed as means ± S.E.M. of n=6-7 hearts.

Hypertrophic hearts from SHR were more susceptible to ischaemia than control hearts from WKY. Recovery (%) in cardiac output (CO, aortic flow + coronary flow) was 76 ± 7 vs. 37 ± 3 for WKY and SHR respectively ($p<0.01$, unpaired t test). Glutamate significantly improved recovery of CO in SHR hearts (68 ± 7%, $p < 0.05$ vs. untreated SHR, unpaired t test), but did not affect WKY hearts (82 ± 7%,). Similarly, total release of LDH (IU/g dry weight) during the first ten minutes of reperfusion was higher in untreated SHR (9.9 ± 0.7, $p<0.05$, unpaired t test) compared to WKY (4.9 ± 0.6) and was significantly reduced with glutamate in the SHR (6.7 ± 0.9, $p<0.05$ vs. untreated SHR, unpaired t test) but not WKY (6.3 ± 1.8).

In conclusion, this work shows that the increased expression and activity of glutamate transporters in hypertrophic hearts is associated with improved recovery of hypertrophic (SHR) rat hearts but not their corresponding control (WKY) hearts following normothermic global ischaemia and reperfusion in the presence of low concentration of glutamate.

Javadov SA *et al.* (2000). *Cardiovasc Res* **45**, 360-369.

King N *et al.* (2004a). *J Physiol* **556**, 849-858.

King N *et al.* (2004b). *J Physiol* **557P**, 25P.

Suleiman M-S *et al.* (1998). *J Mol Cell Cardiol* **30**, 2519-2523.

Supported by the BHF.

Where applicable, the experiments described here conform with Physiological Society ethical requirements.

C72

Optical recording of drug-induced action potential prolongation in isolated cardiac myocytes using a voltage-sensitive dye

M.E. Hardy[1], C.L. Lawrence[2], N.B. Standen[1] and G.C. Rodrigo[1]

[1]Cell Physiology and Pharmacology, University of Leicester, Leicester, UK and [2]Safety Assessment UK, AstraZeneca, Macclesfield, Cheshire, UK

The cardiac action potential results from a complex interplay of voltage-dependent ion channels, pumps and transporters. In this study we have used a fast potentiometric dye to record changes in the morphology of the action potential in response to cisapride, which is known to cause action potential prolongation. Ventricular myocytes, isolated from humanely killed adult guinea pigs, were loaded with 5 uM di-8-ANEPPS for 20 min. Switch clamp experiments, using a patch electrode, were used to confirm that changes in the fluorescence emission ratio from di-8-ANEPPS had a linear relationship with membrane potential between −80 mV and + 60 mV. Averages of 20 traces of optical recordings were used to increase signal: noise ratio. Control values of the action potential duration to 90% repolarization (APD_{90}) measured optically (355 ± 11 ms, mean ± S.E.M) were significantly longer in duration than those recorded using a microelectrode (301 ± 14 ms; $p<0.01$, n = 10, Student's t test). Acute perfusion of 5 uM di-8-ANEPPS shows a maximal increase in APD_{90} of 16 ± 4%, suggesting that the increase in APD observed during optical recording may result from the loading of the dye. Comparisons between action potentials recorded simultaneously both optically and using a patch electrode reveal that the optical measurements are essentially identical to those recorded electrically.

Cisapride, which is known to block I_{Kr}, caused increases in APD_{90} at concentrations of 10-300 nM. However, at 1000 nM cisapride APD_{90} values were shorter than at 300nM, suggesting additional effects of the drug. Increases in APD_{90} at 300nM cisapride compared to control values were 7.7 ± 2.3% when recorded optically and 10.9 ± 2.0% when recorded using a microelectrode (NS). EC_{50} values calculated from dose-response curves were 91 ± 46 nM when recorded optically, compared to 81 ± 20 nM when recorded using an electrode (NS).

These data suggest that guinea pig ventricular myocytes loaded with Di-8-ANEPPS have a longer basal APD, so that cisapride-induced action potential prolongation may be less pronounced when recording optically with this dye, when compared with recordings using a microelectrode. Therefore, optical studies using di-8-ANEPPS may underestimate the arrhythmogenic potential of compounds. However, monitoring cardiac APD in single cells with the use of a voltage-sensitive dye may be feasible for use as an assay.

This work was funded by BBSRC and Astra Zeneca.

Where applicable, the experiments described here conform with Physiological Society ethical requirements.

C73

Gap junctional permeability to protonated mobile buffer shows a biphasic relationship with intracellular pH

P. Swietach and R.D. Vaughan-Jones

University Laboratory of Physiology, University of Oxford, Oxford, UK

Under nominally CO_2/bicarbonate-free conditions (Hepes-buffer), proton transmission between cardiomyocytes occurs by means of protonated mobile buffers passively permeating gap junctions. Ventricular myocytes isolated from humanely killed guinea-pigs were AM-loaded with the pH-sensitive dye, carboxy-SNARF-1, and superfused with Hepes-buffered Tyrode solution (37°C) while imaging pH_i confocally. It has been shown (Swietach & Vaughan-Jones, 2004) that the apparent junctional permeability constant (P_H^{app}) can be calculated from the longitudinal pH_i gradient that is established when a cell-pair is partially exposed to a weak acid or weak base. Using a double-barrelled micropipette, end-to-end cell-pairs were dually microperfused with two microstreams, one of which contained 20-30mM ammonium or 80-120mM acetate. 30μM cariporide was included in both microstreams to block sarcolemmal Na^+-H^+ exchange. Exposure of the distal end of one cell produced a large pH_i gradient in the cell-pair that was maintained for the duration of dual microperfusion. P_H^{app} was estimated from the discontinuity of the longitudinal pH_i profile that coincided with the junctional region. To examine the pH_i-dependence of P_H^{app}, the pH_i of the cell-pair was adjusted to different values (by prepulsing uniformly with extracellular ammonium or acetate) before applying the dual microstream. P_H^{app} was maximal ($5.17(\pm0.23)\times10^{-4}$ cm/s, N=14) at pH 7.0 and declined significantly ($P<0.05$) at both higher and lower pH_i ($2.20(\pm0.38)\times10^{-4}$ cm/s at pH 7.36, N=13 and $1.72(\pm0.48)\times10^{-4}$ cm/s at pH 6.33, N=8). In the presence of reduced extracellular Ca^{2+} (from 2mM to 0.5mM) and increased intracellular Ca^{2+} buffering (by preloading cells with 100μM BAPTA-AM), the maximum P_H^{app} did not change significantly ($4.60(\pm0.49)\times10^{-4}$ cm/s at pH 6.92, N=17), and P_H^{app} was again reduced at both higher and lower pH_i ($2.16(\pm0.59)\times10^{-4}$ cm/s at pH 7.30, N=5 and $2.87(\pm0.43)\times10^{-4}$ cm/s at pH 6.39, N=10). The reduction of P_H^{app} with acidosis under these conditions was, however, significantly smaller than the reduction under normal conditions ($P<0.05$), suggesting that during intracellular acidosis, gap junctions may be closed by a combination of raised $[H^+]_i$ and $[Ca^{2+}]_i$. Gating in the alkaline direction, on the other hand, appears to be $Ca^{2+}{}_i$-independent. Such gating will influence the local spread of acid or base within the myocardium.

Swietach & Vaughan-Jones (2004). Am J Physiol 287, 726-35.

This work was supported by a British Heart Foundation Programme Grant (RDVJ).

Where applicable, the experiments described here conform with Physiological Society ethical requirements.

C74

Distribution of transgenic mRNA in the hearts of transgenic mice expressing GFP-tagged Kir6.2 and Kir2.1 K^+ channel subunits

H. Dobrzynski[1], I.G. Greener[2], T.P. Flagg[3], J.O. Tellez[1], N.J. Chandler[2], A.N. Lopatin[4], C.G. Nichols[3], M.R. Boyett[1] and R. Billeter[2]

[1]Division of Cardiovascular & Endocrine Sciences, Manchester University, Manchester, UK, [2]University of Leeds, Leeds, UK, [3]Washington University, St Louis, MO, USA and [4]University of Michigan, Ann Arbor, MI, USA

In heart, Kir6.2 is responsible for the ATP-sensitive K^+ current (I_{KATP}) and Kir2.1 is in part responsible for the background inward rectifier K^+ current (I_{K1}). In this study, transgenic mice expressing either GFP-tagged Kir6.2 or Kir2.1 K^+ channel subunits under the control of the cardiac α-myosin heavy chain (α-MHC) promoter were generated. We have investigated the distribution in humanely killed mice of Kir6.2-GFP and Kir2.1-GFP mRNA in the sinoatrial node (SAN), compact atrioventricular node (AVN), His bundle, and working myocardium from these transgenic mice. Digoxigenin labelled sense and anti-sense riboprobes were made specific for GFP, and in situ hybridisation was carried out on 10 μm tissue sections mounted on glass slides. We observed that Kir6.2-GFP mRNA was expressed in the SAN (n=3), atrium (n=3) and ventricle (n=3) of transgenic hearts, but was absent in the compact AVN (n=3) and His bundle (n=3). Kir2.1-GFP mRNA was expressed in the atrium (n=3) and ventricle (n=3), but was absent in the SAN (n=3), compact AVN (n=3) and His bundle (n=3). No Kir6.2-GFP and Kir6.2-GFP mRNA was observed in tissue sections from non-transgenic mice from the same litter. The presence or absence of Kir6.2-GFP and Kir2.1-GFP mRNA in the SAN, AVN, His bundle, atrium and ventricle faithfully follows the presence or absence of Kir6.2-GFP and Kir2.1-GFP proteins in these heart tissues. These patterns do not correspond to the expected distribution of α-MHC mRNA, whose core promoter was used in the construct. They do, however, largely correspond to the expected distribution of Kir6.2 and Kir2.1 mRNA and protein in the SAN, AVN and His bundle. This suggests transcriptional regulation of the genes, i.e. control at the level of the transcript, leading to directed exclusion of both transcript and protein from the specific conducting tissues. This may be an important mechanism controlling the expression of the wild-type Kir6.2 and Kir2.1 genes.

Where applicable, the experiments described here conform with Physiological Society ethical requirements.

C75

A swelling-activated outwardly rectifying chloride channel in human atrial cardiomyocytes

M. Demion, R. Guinamard, A. El Chemaly, M. Rahmati and P. Bois

IPBC, University of Poitiers, UMR CNRS 6187, Poitiers, France

Properties of the swelling-induced chloride current ($I_{Cl,swell}$) in cardiac tissue are well known at the macroscopic level. The current is implicated in cell-volume regulation and in pathologies such as myocardial ischemia and dilated cardiopathies. Its main characteristics are a selectivity sequence of $I^- > Br^- > Cl^- > F^-$ > gluconate, outward rectification, and activation by cell swelling. While a macroscopic chloride current with similar properties has been identified in human atrial cardiomyocytes, no study has been realized at the single channel level.

Myocardium specimens were obtained from patients undergoing cardiac surgery according to the European Community Council Directive. Sinus rhythm was present in all cases. Cells were obtained by both enzymatic and mechanical dissociation. Using the cell-attached and the inside-out configurations of the patch-clamp technique, we characterized the properties of an outwardly rectifying chloride current (ORCC) at the unitary level in freshly isolated human atrial cardiomyocytes. In inside-out configuration, under symmetrical conditions (in mM: 140 NaCl, 4.8 KCl, 1.2 $MgCl_2$, 10 glucose and 10 HEPES, with 1 and 1.8 $CaCl_2$ in the pipette and the bath, respectively), the current-voltage relationship shows an outward rectification, 76.5 ± 14.7 pS and 8.1 ± 2 pS in the positive and negative voltage range, respectively (mean ± S.E.M., n = 5). The channel was chloride selective ($P_{Cl}/P_{Na} = 18$) with the permeability sequence $I^- > Br^- > Cl^- > F^-$ > gluconate ($P_I/P_{Cl} = 2.31$, n = 4; $P_{Br}/P_{Cl} = 1.2$, n = 5; $P_F/P_{Cl} = 0.33$, n = 4; $P_{gluconate}/P_{Cl} = 0.27$, n = 4). In our conditions neither $[ATP]_i$ nor $[Ca^{2+}]_i$ had effect on channel activity. The channel activity was decrease by the classical Cl^- channels blockers. Intracellular NPPB (5-nitro-2(-3-phenolpropylamino)benzoic acid) at 1 and 10 μM, SITS at 1 mM and DIDS at 100 μM reversibly reduced the channel activity to 63.1 ± 12.2% ($p<0.05$, n = 5) and 52.3 ± 13.1% ($p<0.01$, n = 5), 28.6 ± 14.5% ($p<0.01$, n = 5) and 60.3 ± 12.2% ($p<0.05$, n = 5) of control, respectively. The glibenclamide was also effective in blocking ORCC. EC_{50} was estimated at 21.5 μM. ORCC detection increased after phorbol-12 myristate, 13-acetate (PMA) treatment, a PKC activator. ORCC activity was detected in 20% of patches (n = 35) in control condition and in 40% (n = 80) after 10 min treatment with 500 nM PMA ($p<0.05$).

On cell-attached patches, bathing cells with hypotonic solution (causing cell swelling) increased channel detection (3.2%, n = 31 vs 76.5%, n = 17; $p<0.01$).

Thus, the ORCC recorded at the single channel level possesses properties of the macroscopic $I_{Cl,swell}$ reported in human atrial myocytes and as such should be considered a major component underlying this current. The human atrial ORCC shows similar properties with ORCC described by Duan et al. (1997) in rabbit atria.

Duan D *et al.* (1997). *Circ Res* **80**, 103-113

Where applicable, the experiments described here conform with Physiological Society ethical requirements.

C76

Evidence for direct modulation by oxytocin of guinea-pig ventricular myocyte electrophysiology

J.C. Hancox, V.K. Pabbathi, Z. Gao, J.T. Milnes and A.F. James

Physiology, University of Bristol, Bristol, UK

Endogenous oxytocin is known to produce a range of physiological actions through its G-protein-coupled receptor (Gimpl

& Farenholz, 2001). Due to its uterotonic effects, oxytocin is also given clinically as an intravenous bolus to minimise bleeding during surgical curettage; it has recently been associated with prolongation of the QT interval of the electrocardiogram when given in this fashion (Charbit et al. 2004). Therefore, the present study was conducted to determine whether or not oxytocin exerts a direct modulatory effect on ventricular cardiomyocyte electrophysiology. Guinea-pigs were humanely killed and ventricular myocytes isolated from the hearts by enzymatic and mechanical dispersion. Recordings were made from ventricular myocytes using the whole-cell patch-clamp recording technique at 37°C (pipette dialysate was potassium-based except for sodium-calcium exchange current measurements). Isolated cells were superfused with a standard Tyrode solution, and with Tyrode solution to which oxytocin (10nM) was added. Application of oxytocin resulted in a prolongation of action potential duration at 90% repolarisation (APD_{90}) by 10.4 ± 2.1% (mean ± S.E.M.; n = 7 cells). Under whole cell voltage-clamp, oxytocin was seen to increase amplitude of L-type calcium current ($I_{Ca,L}$) at +10 mV by 40.1 ± 8.4% (n = 6 cells). Sodium-calcium exchange current (I_{NaCa}) was measured as Ni-sensitive difference current during a voltage-ramp protocol, under conditions in which overlapping currents were inhibited (e.g. Zhang et al. 2001). Oxytocin augmented both inward and outward I_{NaCa} (current at +60 mV was increased by 57.4 ± 14.6%; n= 5 cells). These findings demonstrate that oxytocin can modulate ventricular APD_{90}, $I_{Ca,L}$ and I_{NaCa}.

Charbit B *et al* (2004) *Clin Pharmacol Ther* **76**, 359-364

Gimpl and Farenholz (2001) *Physiological Reviews*, **81**, 629-683.

Zhang YH *et al* (2001) *Cell Calcium* **30**, 351-360.

We thank the British Heart Foundation for financial support.

Where applicable, the experiments described here conform with Physiological Society ethical requirements.

C77

Modelling the effects of acute myocardial ischemia on transmural electrophysilogical heterogeneity, excitation conduction and characteristics of ECG

H. Zhang[1], P. Ward[1], J. Stott[1], T. Tao[1], J.C. Hancox[2] and A.V. Holden[3]

[1]Biological Physics, The University of Manchester, Manchester, UK, [2]Department of Physiology, The University of Bristol, Bristol, UK and [3]School of Biomedical Sciences, The University of Leeds, Leeds, UK

Acute myocardial ischaemia is associated with fatal cardiac arrhythmogenesis. In this study we computed the effects of the ischaemia induced changes of cellular ionic and metabolic conditions on ventricular electrophysiology - transmural heterogeneity, excitation conduction patterns, and characteristics of ECG.

The Luo-Rudy dynamical model (LRd) of electrical action potential (AP) of guinea-pig ventricular myocytes was modified to incorporate the ischaemia induced changes on cellular membrane ionic currents and intra- and extra-cellular K+ ion concentrations [1]. These changes include (1) the elevation of the extra-cellular K+ concentration ([K+]o was set to 12 mM); (2) intra-cellular and extra-cellular acidosis (pH was set to 6.5) that reduces the maximal conductance of the L-type Ca2+ and Na+ channels by 25% respectively. A depolarising shift of the Na+ channel kinetics (by 3.4 mV) and a decrease in [K+]i (set to 125 mM) caused by extra-cellular acidosis were also included; 3) activation of IK(ATP) current produced by a decrease in [ATP]i (set to 3.0 mM) associated with anoxia and metabolic blockade. The modified cell model was then incorporated into a one-dimensional partial differential equation (PDE) model of transmural ventricular strand that incorporates the regional differences of electrical AP and sensitivity of IK(ATP) to [ATP]i. Transmural heterogeneity was quantified by the dispersions of APD90 and cell membrane potentials under normal and ischaemia conditions. Characteristics of computed pseudo-ECG, such as the width of QRS complex, QT time interval and the width and amplitude of the T-wave were also quantified.

Simulations of ischaemia-induced changes on cellular ion channel kinetics and metabolic condition abbreviate ventricular AP with greater effects on epicardial (EPI) and midmyocardial (MID) cells than the endocardial (ENDO) cell. This attenuated rather than augmented the transmural dispersions of measured APD90 and cell membrane potentials. There was a significant increase in the width of the QRS complex in the computed pseudo-ECG (changed from 18 ms in normal to 34 ms in ischaemia conditions), which indicated a dramatic slowing down of transmural ventricular excitation conduction. Ischaemia shortened the QT time interval (changed from 153 ms in normal to 98 ms in ischaemia conditions) and the width of the T-wave. The measured time interval between the peak of the T-wave (Tp) and the end of the T-wave (Te) decreased from 34 ms in normal condition to 22 ms in ischaemia condition.

Under our simulation conditions global acute myocardial ischaemia does not augment the transmural heterogeneity of ventricular electrophysiology, but does lead to a shortened QT interval.

RM Shaw, Y Rudy (1997) Cardiovascular Res 35: 256-272

Supported by grants from the BHF, EPSRC and EU Network BioSim(contract number 005137)

Where applicable, the experiments described here conform with Physiological Society ethical requirements.

C119

Slow conduction in mouse hearts with targeted disruption of the cardiac sodium channel gene, Scn5a

G. Xiao[1], S. Paulich[2], C.A. Goddard[3], W.H. Colledge[3], A.A. Grace[3], C.L. Huang[3] and M. Lei[2]

[1]Dept of Cardiovascular Medicin, Union Hospital, Tongji Medical College, HUST, Wuhan, China, [2]Physiology, University of Oxford, Oxford, UK and [3]Depts of Biochemistry and Physiology, University of Cambridge, Cambridge, UK

In patients, loss-of-function mutations of the cardiac sodium channel gene, SCN5A, have been associated with a wide range of arrhythmias including bradycardia, atrioventricular conduction delay, and ventricular fibrillation (Papadatos et al. 2002). The pathophysiological basis of these conditions has not been fully understood. We examined cardiac conduction properties in mice with a targeted disruption of the cardiac sodium channel gene.

Adult wild-type mice and mice with a targeted disruption of the cardiac sodium channel gene Scn5a (Scn5a+/-) were humanely killed. The hearts were removed and were Langendorff-perfused with Tyrode solution at a flow rate of 3.8 ml/min at 37°C. Electrocardiogram was first recorded on Langendorff-perfused hearts by custom-made electrodes to measure P-P (representing cycle length and heart rate) and PR interval (representing intraatrial and atrioventricular nodal conduction). A preparation containing the sinoatrial node, atrio-ventricular node and part of the right atrium and ventricle was dissected. The preparation was then fixed in a tissue bath and superfused with Tyrode solution at 37°C at a rate of 4 ml/min through a heat exchanger into chamber. Extracellular potentials (ECPs) were recorded by two bipolar electrodes from the preparations as described by Lei et al. (2004). Data are expressed as means ± S.E.M. (number of preparations or cells). Differences were evaluated by Student's unpaired t test with a P value <0.05 considered significant.

Scn5a+/- hearts showed depressed heart rates (260 ±25 beats/min, n=6) and frequent atrioventricular (A-V) block compared with wild type (WT) hearts (335 ± 19 beats/min, n=6, P<0.05 vs WT). Scn5a+/- preparations exhibited significantly longer sinoatrial conduction time (SACT: 11 ± 2 ms, n=6, P<0.01 vs WT) and sino-ventricular conduction time (S-VCT: 13.6 ± 1.0 ms, n=6, P<0.05 vs WT) compared with WT preparations (SACT: 5 ± 1 ms; S-VCT: 10.7 ± 1.6 ms). Applications of TTX at 1 and 5 μM prolonged SACT by 22 ±7 and 39 ± 4%, respectively, in WT preparations (n=5) and by 30 ± 5 and 56 ± 9% (n=5, P<0.01 vs WT) in Scn5a+/- preparations, suggesting Scn5a+/- preparations are more sensitive to TTX.

The results show that Scn5a is involved in normal sino-atrial and atrio-ventricular conduction and reduction of sodium channels can cause cardiac conduction system dysfunction.

Lei M et al. (2004). J Physiol 559, 835-848.

Papadatos GA et al. (2002). PNAS 99, 6210-6215.

The study was supported by the Wellcome Trust and Chinese NSF grant.

GS Xiao and S Paulich contributed equally to the study.

Where applicable, the experiments described here conform with Physiological Society ethical requirements.

C120

HCN channels and mouse atrioventricular node pacemaking

J. Liu[1], M. Abdelrahman[1], G. Xiao[1], H. Dobrzynski[2], M.R. Boyett[2] and M. Lei[1]

[1]Physiology, Oxford University, Oxford, UK and [2]Cardiovascular and Endocrine Sciences, University of Manchester, Manchester, UK

The atrioventricular node (AVN) serves not only as the exclusive conduction pathway between the atrium and ventricles, but also as a secondary pacemaker in the event of sinoatrial node (SAN) failure. To investigate the mechanism underlying pacemaking in the mouse AVN, the expression of hyperpolarization-activated, cyclic nucleotide-gated (HCN) channels (responsible for I_f current) were studied in the AVN (as well as the SAN).

Hearts were excised from humanely killed 20-25 g adult C57BL mice. The AVN with some surrounding tissue was dissected from the right atrioventricular junction at the triangle of Koch. The preparation was fixed in a tissue bath and superfused with Tyrode solution and extracellular potentials were recorded as described by Lei et al. (2004) (1). After electrical recording, tissue was frozen and sectioned, and histological and immunohistochemical studies were carried out as described by Lei et al. (2004) (1). Images were acquired by a Zeiss LSM5 PASCAL confocal microscope and analysed by Image J software. Data are presented as means ± SEM (number of preparations). Differences were evaluated by Student's t test and a difference was considered significant if $p<0.05$.

To confirm the functional role of I_f in mouse AVN, the effect of 0.5 mM Cs^+ (blocker of I_f) on the spontaneous pacemaker activity of the isolated AVN preparations was examined. Cs^+ prolonged the cycle length (CL; time between spontaneous action potentials) by 122% from 252 ± 53 ms under the control conditions to 560 ± 154 ms in the presence of Cs^+ (n=5, $p<0.01$). In contrast, Cs^+ prolonged the CL of the SAN by just 15%. After washing off Cs^+ for 5 to 10 min, spontaneous AVN rhythm recovered fully. Immunostaining was carried out using antibodies against HCN isoforms. There was no labelling of HCN1 in the AVN and SAN. There was non-myocyte labelling of HCN2 in the AVN and SAN. There was punctate membrane labelling of HCN4 in the myocytes of the AVN and SAN, but the labelling intensity in the AVN was ~20% of that in the SAN.

Based on the effect of Cs^+ on the spontaneous activity of the AVN and SAN (and also preliminary data obtained with the I_f blocker, ZD7288), we conclude that I_f plays a more important role in the pacemaking of the AVN than the SAN. Based on the immunostaining, we conclude that HCN4 is the major isoform responsible for I_f in the mouse AVN and SAN and, paradoxically, HCN4 is more abundant in the SAN than AVN.

Lei M et al. (2004). J Physiol 559, 835-848.

The study was supported by the Wellcome Trust.

Where applicable, the experiments described here conform with Physiological Society ethical requirements.

C121

Characteristics of the short QT syndrome-linked HERG mutation N588K

M.J. McPate, R.S. Duncan, J.T. Milnes, H.J. Witchel and J.C. Hancox

Physiology, University of Bristol, Bristol, UK

The idiopathic short QT syndrome (SQTS) is characterised by abbreviated QT intervals on the electrocardiogram and an increased risk of cardiac arrhythmia (Gussak et al, 2002). Recently, one form of SQTS has been linked to two different missense mutations in *HERG (Human ether-a-go-go-related gene)* leading to a common amino-acid substitution (N588K; asparagine to lysine) in the S5-Pore linker region of the HERG channel (Brugada et al, 2004). Data from recordings at ambient temperature of heterologously expressed N588K channels suggest that this amino acid change results in a loss of voltage-dependent inactivation and a consequent gain in HERG channel function (Brugada et al, 2004). The present study was conducted in order to determine characteristics of N588K channel current at a physiological temperature. The N588K mutation was made by a two-primer PCR approach and recombinant N588K-HERG channels were transiently expressed in Chinese Hamster Ovary (CHO) cells. Whole-cell patch-clamp recordings were made at 37ºC, using a potassium-based pipette dialysate. Two second duration voltage-clamp commands were applied from −80 mV to a range of test potentials in 10 mV increments. The end-pulse current-voltage relation for wild-type (WT) HERG current (I_{HERG}) was compared with that for N588K-HERG. WT I_{HERG} was maximal at ~0 to +10 mV and declined at more positive voltages (n = 5 cells). In contrast, within a physiologically relevant range of test potentials (up to ~ + 40 mV), N588K I_{HERG} continued to increase with progressive depolarisation (n = 5 cells). However, depolarisation to a highly positive voltage (+100 mV) resulted in a marked decline in I_{HERG} amplitude compared to + 40 mV ($P<0.01$; paired *t* test; n = 4 cells). These observations provide evidence that the N588K mutation does not eliminate I_{HERG} inactivation entirely, but rather shifts normal I_{HERG} rectification towards more positive voltages.

Brugada R *et al* (2004) *Circulation* **109**, 30-35

Gussak I *et al* (2002) *Card Electrophysiol Rev* **6**, 49-53

This work was funded by the British Heart Foundation

Where applicable, the experiments described here conform with Physiological Society ethical requirements.

C122

Voltage-dependent changes in affinity characterise preferential closed state blockade of HERG by BeKm-1 and Ergtoxin

J.T. Milnes[1], C.E. Dempsey[2], J.M. Ridley[1], J.C. Hancox[1] and H.J. Witchel[1]

[1]Physiology, University of Bristol, Bristol, UK and [2]Biochemistry, University of Bristol, Bristol, UK

Previous work has shown that the fractional blockade of the HERG potassium channel by the scorpion toxin BeKm-1 has a negative dependence on voltage, and strong depolarisation of the cell membrane can eliminate this blockade (Milnes et al. 2003; Zhang et al. 2003). These studies arrived at contradictory conclusions regarding whether or not the mechanism of block involves voltage-dependent changes in BeKm-1's affinity for the channel. Here we used whole-cell patch-clamp at 37°C of HEK 293 mammalian cells expressing heterologous HERG to show that the time course of development (τ) of channel blockade after repolarisation of the membrane varies from 1404 ± 25 ms (mean ± S.E.M.) at 50 nM BeKm-1 to 384.2 ± 0.2 ms at 500 nM ($P < 0.001$, ANOVA with Bonferroni post-test, n = 6-15); furthermore, at these two concentrations the τ of blockade following repolarisation to 0 mV is identical to the τ of blockade following rapid wash on of BeKm-1 while the membrane is held at 0 mV (not significant, ANOVA with a Bonferroni post-test). We also found that 500 nM of BeKm-1 results in highly potent block (95.00 ± 0.03%, n = 5) when tail currents (-40 mV) were measured after a short (30 ms) depolarisation to +40 mV, although prolonging the depolarizing pulse to 210 ms resulted in significant time-dependent reduction in block by 500 nM BeKm-1 (ANOVA, $P <0.001$); this is compared with previous results suggesting that maximal blockade of HERG by BeKm-1 does not approach 100% (Zhang et al. 2003). In addition, strong depolarisation (+80 mV for 3 s) can result in an acceleration of toxin wash-off from the channel when held at -80 mV for a further 7 s ($P < 0.001$, ANOVA with a Bonferroni post-test, n = 6-9 cells). Finally, strong depolarisation can lead to apparent switching from block by Ergtoxin to block by BeKm-1 (as judged by time course) when in the presence of both toxins ($P < 0.001$, n = 4-6). These data are concordant with voltage-dependent changes in HERG's affinity for the two toxins, and the data diverge from a model in which the toxin is continuously resident in its binding site on the channel in a voltage-independent manner.

Milnes JT et al. (2003). *FEBS Lett* **547**, 20-26.

Zhang M et al. (2003). *Biophys J* **84**, 3022-3036.

We gratefully acknowledge the support of the British Heart Foundation (PG/2001104 and PG/2000123) and the Wellcome Trust (Fellowship to J.C.H.).

Where applicable, the experiments described here conform with Physiological Society ethical requirements.

C123

Functional overexpression of TRPM4-like cationic current on spontaneously hypertensive rats

R. Guinamard, M. Demion, C. Magaud, A. El Chemaly and P. Bois

IPBC, university of Poitiers, UMR CNRS 6187, Poitiers, France

Cardiac hypertrophy is associated with electrical modifications, including sustained depolarisation and modification of action potential, that lead to a propensity for arrhythmias. Ionic currents such as I_f, $I_{Ca\text{-}T}$ and I_{to} participate in these modifications. In addition, we previously reported the appearance of a Ca^{2+}-activated non-selective cation current (NSC_{Ca}) in adult cardiomyocyte culture, which has been proposed as an in vitro model of cardiac hypertrophy (Guinamard *et al.* 2002). In the

same way, we report in the present study, an enhanced expression of this current on freshly isolated cells from spontaneously hypertensive rats (SHR) known to develop cardiac hypertrophy. Cells were isolated from the left ventricles of hearts from 3 to 6 month old Wistar Kyoto or SHR male rats using both enzymatic and mechanical dissociation processes. Animals were humanely killed in accordance with the European Community Council Directive. Before patching, cells were incubated for at least 10 min with 500 nM phorbol 12-myristate, 13-acetate (PMA), a PKC activator that activates the cardiac NSCCa (Guinamard *et al.* 2004). Channel activity was recorded in inside-out patches with a solution (bath and pipette) containing (mM): 140 NaCl, 4.8 KCl, 1.2 $MgCl_2$, 1 $CaCl_2$, 10 glucose and 10 Hepes. In these ionic conditions, the channel exhibited a linear current-voltage relationship ($\gamma = 23.3 \pm 1.1$ pS, n = 4). Channel activity increased with depolarisation. Open probability as a function of voltage was fitted to a Boltzmann function with values of 15.5 for s and +43.8 mV for $V_{0.5}$. The channel discriminated poorly among monovalent cations (Na^+, K^+) and was impermeable to Cl^- ($P_{Cl}/P_{Na} = 0.08$). Reducing internal calcium to 10^{-9} M abolished channel activity. These properties are similar to those previously reported on dedifferentiated rat ventricular myocytes (Guinamard *et al.* 2002).

NSC_{Ca} channel activity, which was rarely detected in cardiac cells from normotensive rats (7.3% of patches, n = 41) even after PMA treatment was frequently recorded in myocytes from SHR rats (43.8% of patches, n = 16).

Cardiac hypertrophy was associated with a prolongation of the QT interval on the ECG. The increase in NSC_{Ca} channel occurrence observed during cardiac hypertrophy, which increased the Na^+ influx, would participate in slowing repolarisation. In addition, activation of the channel will be able to modify the resting membrane potential to a less negative value leading to more excitable cells. Thus the NSC_{Ca} may play a primary role in the genesis of arrhythmias. The NSC_{Ca} channel shares the hallmarks of the TRPM4 channel (Launay et al. 2002).

Guinamard R *et al.* (2002). *J Memb Biol* **188**, 127-135.

Guinamard R *et al.* (2004). *J Cardiovasc Electrophysiol* **15**, 342-348.

Launay P *et al.* (2002). *Cell* **109**, 397-407.

Where applicable, the experiments described here conform with Physiological Society ethical requirements.

C124

Metabolic substrates affect differently contractility of left ventricular cardiomyocytes in pregnancy and in experimental preeclampsia in rats

V. Bassien-Capsa, B. Comte and A. Chorvatova

Sainte Justine Hospital, Centre de recherche, Montreal, QC, Canada

Preeclampsia, a hypertensive disorder during pregnancy, is associated with important risks for maternal and perinatal morbidity and mortality. Notwithstanding, cardiac changes in this condition are still poorly understood. Significant modifications in carbohydrate metabolism are induced in pregnancy to provide continuous nutrients availability to the developing fetus, primarily depending on glucose. Our objective is to identify how metabolic changes, taking place during pregnancy, affect the cardiomyocyte function in late stages of normal pregnancy and of experimental preeclampsia induced by a high sodium intake (Auger et al. 2004).

Two groups of Sprague-Dawley pregnant rats were studied. The first received tap water (P) and was compared with non-pregnant females (NP). The second received 0.9% NaCl to drink for the last 7 days of pregnancy (P0.9) and was compared with P. At the 21st day of pregnancy, rats were humanely killed, blood collected for metabolite assays and single left ventricular myocytes isolated. Contractility was assessed by confocal microscopy. Data are shown as mean ± S.E.M. (n).

First, we compared blood levels of glucose, lactate and pyruvate ($p<0.05$ P vs NP and P0.9 vs P using a factorial ANOVA). In P, there was a significant decrease in glycaemia from 16.2 ± 0.8 mM (5) to 9.0 ± 1.4 mM (5), in accordance with glucose being used by the fetus. Significantly increased lactate levels led to a rise in the lactate/pyruvate ratio from 18.8 ± 1.8 (5) to 26.4 ± 1.9 (5), indicating redox state modifications. In P0.9, compared with P, neither levels of glucose, nor lactate and pyruvate were significantly different, but the lactate/pyruvate ratio failed to increase, remaining at 20.3 ± 1.4 (5).

Second, cells were exposed, additionally to glucose, to blood levels of the carbohydrate substrates and/or octanoate, a medium chain fatty acid, and cell contractility was assessed.

Figure 1 shows that in pregnancy (P and P0.9), contrary to NP, the addition of substrates significantly affected cell shortening (0.5 Hz, 35 ± 1°C) when compared to the condition with glucose only ($p<0.05$ vs P using a factorial ANOVA). In P0.9, the effect of lactate was blunted when compared to P. The pattern of the response was parallel when the experiments were performed at 6 Hz (not shown), suggesting that this phenomenon is not frequency dependant.

Our data indicate that adaptations in the use of metabolic energy substrates occur in normal pregnancy and that this process is impaired in experimental preeclampsia.

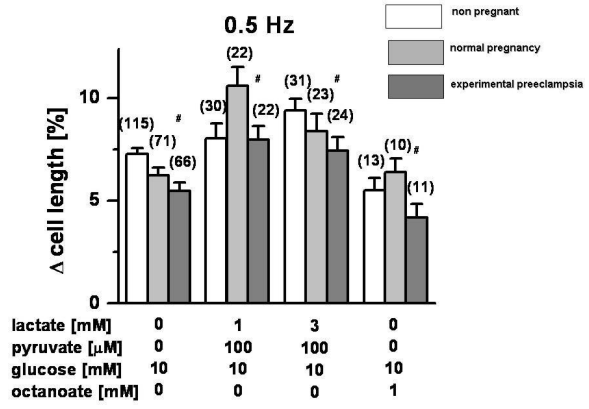

Figure 1. Effect of substrates on cell shortening

Auger K et al. (2004). Am J Physiol 287, H1848-1856.

The work was supported by Canadian Institutes of Health Research MOP 74600.

Where applicable, the experiments described here conform with Physiological Society ethical requirements.

PC1

Investigating intracellular proton mobility and junctional proton transmission using photolytic uncaging of proton donors

P. Swietach and R.D. Vaughan-Jones

University Laboratory of Physiology, University of Oxford, Oxford, UK

The inclusion of 1mM of the membrane-permeant aldehyde, 2-nitrobenzaldehyde (NBA) in superfusion solutions has no major side-effects on rat ventricular myocyte contractility or intracellular pH (pH_i) but does provide substrate for photolytic release of protons by flashes of UV laser light. Myocytes were enzymically isolated from the ventricles of humanely killed rats. Cells and cell-pairs were AM-loaded with the fluorophore carboxy-SNARF-1 or carboxy-SNARF-4F for confocal imaging of pH_i. Whole-cell exposure to a flash of UV light (pixel dwell time 9.8μs) produced a uniform fall of pH_i of ~0.01 pH_i units, equivalent to an acid load of 0.22±0.07 mM (n=7). The release of acid can be confined to a region of interest (as small as 4 by 4μm) to investigate H^+_i mobility by following the relaxation of pH_i after a burst (1Hz for 6s) of UV flashes or by following the progress of acid-loading between consecutive UV flashes (0.1Hz for 60s). Since flash photolysis produces large acid-loads, it can also be adapted to measure junctional transmission of acid between coupled cells. Under Hepes-buffered conditions and in the presence of 30μM cariporide to block sarcolemmal Na^+-H^+ transport, the apparent proton diffusion coefficient (D_H^{app}) at resting pH_i determined by each photolytic method was $13.4\pm1.63\times10^{-7}$ cm^2/s (N=46, burst of flashes) and $12.2\pm1.04\times10^{-7}$ cm^2/s (N=29, continuous flashing), respectively. These were similar to the previously determined value of D_H^{app} using pipette-loading of acid (Zaniboni et al, 2003, Am J Physiol 285, H1236-46). By manipulating starting pH_i (by means of a whole-cell ammonium or acetate prepulse), D_H^{app} was shown to rise four-fold over the pH_i range 6.4 to 7.4. The apparent junctional permeability constant for protons (P_H^{app}) was $1.9\pm0.5\times10^{-5}$ cm/s (N=17) for side-by-side pairs at a mean pH_i of 7.13±0.04. Photolytic uncaging of protons offers a new and less invasive method of studying proton mobility than by using pipette acid-loading. This technique can also potentially be used to study H^+_i mobility in intact myocardium and even perfused hearts. *This work was supported by a British Heart Foundation Programme Grant (RDVJ).*

Where applicable, the experiments described here conform with Physiological Society ethical requirements.

PC2

Generation of muscular cells from mesenchymal stem cells by chemically induced transdifferentiation

C. Bunu, E. Deak, I. Siska, G. Tanasie, V. Ciocotisan and V. Paunescu

Physiology, University of Medicine and Pharmacy Victor Babes, Timisoara, Romania

The aims of the study were to investigate if human adult mesenchymal stem cells (MSCs) can transdifferentiate into muscular cells with specific genetic features, and to analyse if there is a correspondence between the type of stimulation and the amplitude of gene expression.
Cells were extracted after previous filtration and density fractioning of the marrow aspirate. They were seeded and cultured in Iscove's modification of Dulbecco's medium (IMDN) with 20% fetal calf serum (FCS), penicillin and streptomycin, at 37°C in a 5% CO_2 environment. Cultures reaching 80% confluence were reseeded in 24-well plaques and split in two different groups according to the stimulation pattern. Continuous pattern implying maintenance of 5-azacitydine (1,2} in culture for the entire time length and discontinuous pattern implying removal of 5-azacitydine after 24 h followed by another addition after 24 h (6 samples in triplicate for each type of experiment).
Within a 5 week interval of stimulation cultures from both groups underwent morphological changes. Cells begun to entangle developing colonies in which they started to multiply forming layers which gave a tissue-like appearance of the colonies. Round shaped cells, with different morphological features, rose within the colonies by the third week of culture. A decrease in cell density was noticed particularly in the continuously stimulated cultures.
Total RNA was extracted followed by reverse transcription, the resulting cDNA was subjected to quantitative PCR analysis for genes encoding myogenin and myogenic factor 5 (MYF5), both specific for muscular cells (3). As positive controls we used an acute myelogenous leukemia (AML) sample, which highly expresses the two markers. Results showed a more enhanced expression in the continuously stimulated cultures with a peak at 30th cycle versus 35th cycle for both markers, suggesting that the stimulated cells produced a higher amount of specific RNA. The efficiency of RNA extraction and reverse transcription was assessed by glyceraldehyde-3-phosphate dehydrogenase (GAPDH) analysis.
We conclude that 5-azacitydine stimulation induces synthesis of muscular specific RNA in MSCs (3,4). Continuous culture in the presence of 5-azacytidine induces higher gene expression, while discontinuous stimulation allows better cell survival.

Gang EJ et al. (2004). Stem Cells 22, 617-624.

Xu W et al. (2004). Exp Biol Med (Maywood) 229, 623-631.

Fukuda K (2003). Bone Marrow Transplant 32 Suppl 1, S25-27.

Rangappa S et al. (2003). Ann Thorac Surg 75, 775-779.

The study was supported by VIASAN grant no. 311/2004.

Where applicable, the experiments described here conform with Physiological Society ethical requirements.

PC3

Regulation of respiration by calcium in rat heart mitochondria during postnatal development

D. Balaska, L. Brodd, A. Halestrap, S. Suleiman and E. Griffiths

Bristol Heart Institute, Department of Biochemistry, University of Bristol, Bristol, UK

In adult myocytes, mitochondrial respiration is stimulated by an increase in intramitochondrial free calcium ($[Ca^{2+}]_m$), which allows the heart to increase its ATP supply rapidly with changes

in physiological conditions. However, it is not known whether this ability is present from birth, or acquired during development. The aims of this study were to establish whether Ca^{2+} increased respiration rates and 2-oxoglutarate dehydrogenase (OGDH) activity in rat heart mitochondria during postnatal development.

Rats were humanely killed, and mitochondria isolated from hearts of neonatal (2-3 day old), 7, 14, 21 day old, and adult (2-3 month old) male Wistar animals. The rate of respiration was measured by following oxygen consumption of intact mitochondria using an oxygen electrode, and OGDH activity in permeabilised mitochondria by monitoring production of NADH using a spectrophotometric assay. Results are expressed as means ± S.E.M. and statistical significance determined by 1-way ANOVA. n = at least 6 separate preparations of mitochondria.

Using 0.5 mM [2-oxoglutarate], which is rate-limiting in mitochondria from adult rats, 0.6 μM [Ca^{2+}] stimulated respiration approximately 2-fold ($p<0.05$) in mitochondria from adult and 21-day-old rat hearts; but this effect was not observed in the 2, 7, or 14 day olds. However, at 0.1 mM [2-oxoglutarate], 0.6 μM [Ca^{2+}] stimulated respiration in both adult and neonatal mitochondria ($p<0.01$). Thus at 0.5 mM 2-oxoglutarate in the neonates, high rates of respiration were observed even in the absence of [Ca^{2+}]. When OGDH activity was measured, 0.6 μM Ca^{2+} increased enzyme activity in all age groups when either 0.1 or 0.5 mM [2-oxoglutarate] was used. However, kinetic measurements indicated that affinities of the enzyme for its substrate differed: K_m was 0.92 ± 0.15 vs. 0.52 ± 0.06 mM ($p<0.05$), and V_{max} 47.7 ± 5.7 vs. 18.6 ± 3.3 nmol min^{-1} mg^{-1} in adults vs. neonates, respectively. 1 μM Ca^{2+} reduced the K_m of the enzyme from 0.92 ± 0.15 to 0.17 ± 0.01 mM ($p<0.05$) in the adult and 0.52 ± 0.06 to 0.04 ± 0.02 mM ($p<0.05$) in the neonate, without affecting V_{max}.

In conclusion, Ca^{2+} can stimulate respiration at all stages of development, which correlates with activation of OGDH by Ca^{2+}. This suggests the presence of Ca^{2+}-sensitive respiration from birth; however, the higher affinity of OGDH for its substrate may overcome any effect of Ca^{2+} in mitochondria from neonatal rat hearts.

This work was supported by the British Heart Foundation.

Where applicable, the experiments described here conform with Physiological Society ethical requirements.

PC4

Expression of iNOS in preconditioned hearts of aged male rats

A.G. Portnychenko, M.I. Vasylenko and O.O. Moybenko

Experimental Cardiology Department, Bogomoletz Institute of Physiology, NAS of Ukraine, Kyiv, Ukraine

Heart preconditioning characterized by an induction of inducible nitric oxide synthase (iNOS) protein expression mediates cardioprotection from infarction. Myocardial infarction morbidity is known to increase in middle-aged men. The aim of this investigation is to determine whether iNOS protein expression is changed in ischemic hearts of aged male rats with or without preconditioning. 6-, 12- or 18-month-old male Wistar rats were used in the experiments. Preconditioning was induced by whole body hypoxia (10% O_2, 3 h) or whole body hyperthermia (40°C, 10 min). After 24 h, the animals were anesthetized; the hearts were excised and perfused according to the Langendorff mode. After initial stabilization, the isolated hearts were made totally ischemic (30 min) and then reperfused (40 min). The time of ischemic arrest, the time of postischemic heart recovery and the fatal arrhythmia events were registered to estimate a cardioprotection, induced by preconditioning. Protein expression was determined separately in the left and right ventricles of the hearts by Western blotting analysis using BioRad Labs protocols and equipment, and specific polyclonal antibodies from Sigma. The protein expression was estimated by computer densitometry using arbitrary units. It was shown that preconditioning caused induction of iNOS in myocardial tissues. In 6-month-old rats, the iNOS protein expression was 2-fold higher in right ventricles of the hearts than in the left ones. In aged rats (12- and 18-month-old), the expression of iNOS protein decreased 1.1- to 2.0-fold in comparison with 6-month-old rats. During postischemic reperfusion, the hearts of preconditioned 6-month-old rats demonstrated cardioprotective phenomena with limitation of unfavourable iNOS superinduction. However, in the hearts of aged rats was found marked individual differences in the cardioprotection and in the iNOS expression, from slight induction to strong activation like to control, non-preconditioned hearts. At the same time, the insufficient iNOS induction was accompanied by elevated induction of some heat shock proteins (HSP), especially, HSP32, which has iNOS-inhibiting properties. The data presented here have important implications for the validity of hypothesis that disturbances in myocardial induction of iNOS may represent the crucial event in the mechanisms leading to the rise of myocardial infarction events in aged men.

Where applicable, the experiments described here conform with Physiological Society ethical requirements.

PC5

Implication of interactions between cardiomyocytes and cardiac fibroblasts on fibroblast proliferation

C. Louault, S. Fredj, J. Bescond and D. Potreau

UMR 6187 CNRS/Universite de Poitiers, Poitiers, France

The effect of interactions between cardiomyocytes (CM) and cardiac fibroblasts (CF) maintained in primary culture were investigated on CF proliferation. CF cultures and CM/CF cocultures were performed from enzymatically isolated cardiac cells from Swiss mice (2–4 months old) anaesthetized with ether. Fibroblast number was evaluated by counting sarcomeric a-actinin-negative, fibronectin-positive cells. When cultivated alone, CF number per well was increased from day 2 to day 8 of culture (799 ± 248 vs. 1,684 ± 646, respectively; n = 4, $P < 0.01$, two-tailed paired Student's t test) and then remained virtually constant until day 12 (1,563 ± 225, n = 4). Interestingly, there was a significant increase in CF number at the beginning of the culture in the presence of CMs. After 2 days of culture, the number of CFs was increased sevenfold per well in CM/CF cocultures (6,466 ± 1,032, n = 4) compared to CF cultures alone (799 ± 248, n = 4). Thereafter, the number of CFs in coculture with CMs was increased by 40 and 31% at day 8 and day 12, respectively. These

data suggest that the presence of CMs strongly favoured fibroblast adhesion and/or proliferation at the beginning of the coculture which could result from an interaction between the two cell types.

We have shown that interleukin-6 (IL-6) was involved in cardiomyocyte hypertrophy and that IL-6 secretion by CM was potentiated by CF (Fredj et al. 2005). To specify the role of IL-6 on fibroblast proliferation, the effects of IL-6 and gp130 antagonists were investigated. In CM/CF cocultures supplemented with MAB406 (an IL-6 antagonist monoclonal antibody) or AF468 (a gp130 antagonist polyclonal antibody), the number of CFs decreased by 24 ± 15% (n = 3, P < 0.05) and 74 ± 4% (n = 3, P < 0.001), respectively, compared to cultures in which these agents were absent. When cultivated in the absence of CMs, CF number was not significantly modified irrespective of the culture conditions (control medium, 2,466 ± 356 (n = 3); in the presence of anti-IL-6, 2,247 ± 351 (n = 3); in the presence of anti-gp130, 1,817 ± 317 (n = 3)). These data suggest that IL-6 could be involved in fibroblast proliferation, although the strong inhibitory effect of gp130 antagonist indicates that other cytokines of the IL-6 family could also mediate this process.

These results clearly show that fibroblast proliferation is favoured by CM/CF interactions with cytokines of the IL-6 family as autocrine and/or paracrine mediators. It would be interesting to identify other cytokine(s) that may be involved and the role of these interactions on fibroblast differentiation.

Fredj S, Bescond J, Louault C & Potreau D (2005). J Cell Physiol 202, 891–899.

Where applicable, the experiments described here conform with Physiological Society ethical requirements.

PC6

Functional interaction between cardiac sodium-bicarbonate cotransporter and carbonic anhydrase in isolated rat cardiac myocytes

F.C. Villafuerte, P. Swietach, R. Cardenas and R.D. Vaughan-Jones

BSCSC-University Laboratory of Physiology, University of Oxford, Oxford, UK

By using whole-cell pH_i epifluorescence (AM-loaded carboxy-SNARF-1) we evaluated the functional coupling of the Na^+-HCO_3^- cotransporter (NBC) and the Na^+/H^+ exchanger (NHE) with carbonic anhydrase (CA) in ventricular myocytes isolated enzymically from humanely killed Sprague-Dawley rats.

We analysed the pH_i recovery from an acid-load (NH_4^+ prepulse technique) in myocytes superfused with HCO_3^-/CO_2-buffered Tyrode in the presence of cariporide or S0859 to measure the flux mediated by NBC and NHE, respectively. Each set of experiments was carried out in the presence or absence (control) of acetazolamide (ATZ; 100μM), a membrane-permeant CA inhibitor, in order to determine whether the activities of these transporters are functionally coupled to CA.

NHE-mediated flux was not affected by ATZ (n=17). NBC showed a tendency towards lower flux in the presence of ATZ (n=26), particularly at lower pH_i values but without reaching significance. In order to evaluate the effect of ATZ under high NBC flux conditions and over a wider pHi range, we monitored NBC-mediated pH_i recovery in iso-osmotic solutions containing high $[K^+]$ (45mM). This resulted in a marked increase (3.38-fold) of NBC flux over the pH_i range 6.40-6.85. ATZ caused a significant reduction by 51% ± 2 of NBC activity (n=12, p<0.05; unpaired t test).

CA activity in cardiac myocyte lysates was assayed in order to test ATZ potency. Cell lysates were obtained by resuspending ventricular myocytes in 20mM Hepes buffer (pH 8.0 at 4°C) and subsequent sonication. The time courses of pH change at 4°C after addition of 15.6mM CO_2 to lysates +/- 100μM ATZ, and to HEPES-buffer as blank were recorded. CO_2 hydration rates were significanly reduced in the presence of ATZ (n=6, p<0.05; unpaired t test) and were similar to the rate of the un-catalysed reaction, showing that ATZ effectively abolished CA activity in our assay.

Our results show that CA activity does not enhance NBC-mediated acid efflux under normal low-flux conditions. However, under conditions of high NBC activity (e.g. hyperkalaemia combined with low pH_i) CA activity is required to sustain acid extrusion. The enzyme therefore provides a safety mechanism allowing high NBC flux under extreme conditions. This mechanism may be of relevance under conditions associated with acid-overload, such as post-ischaemic reperfusion of the myocardium.

This work was supported by a Wellcome Trust Studentship (F.C.V.) and a BHF Programme Grant (R.D.V.J.).

Where applicable, the experiments described here conform with Physiological Society ethical requirements.

PC7

Thyrotropin-releasing hormone (TRH) release by rat heart

Z. Bacova[1], L. Baqi[2], L. Smrekova[1], O. Benacka[1], J. Payer Jr[1], O. Krizanova[3], J. Payer[2] and V. Strbak[1]

[1]Institute of Experimental Endocrinology, Slovak Academy of Sciences, Bratislava, Slovakia, [2]Department of Internal Medicine, Faculty of Medicine, Comenius University, Bratislava, Slovakia and [3]Institute of Molecular Physiology and Genetics, Slovak Academy of Sciences, Bratislava, Slovakia

Expression of proTRH in the heart has already been shown. Recent data (1) indicate important role of TRH in arterial blood pressure in spontaneously hypertensive rats. TRH can also increase cardiac performance in rats with ischemic cardiomyopathy (2). Thus, in addition to catecholamine and angiotensin II, pro-TRH/TRH may be another important axis that affects hemodynamics and cardiac function (2). It was of interest to show if cardiac tissue could secrete TRH and how this secretion could be controlled.

For in vivo experiments, arterial (a. carotis) and venous (v. jugularis) canula was inserted under Inactin anesthesia (133 mg kg^{-1}) on the day of the experiment. One hour later the animals were injected with 0.5 ml of undiluted specific rabbit TRH antiserum or normal rabbit serum intravenously. Mean arterial blood pressure and heart rate were measured 30 and 90 min later. Hemorrhage (30% of circulating blood volume) was induced by opening the arterial canula at a speed 0.3 ml min^{-1}. Arterial blood pressure and heart rate were than measured immediately after the hemorrhage as well as 60 and 120 min later.

For in vitro experiments the heart was rapidly removed after humane killing of intact adult male rats and tissue from the left auricle (LA) and ventricle (LV) dissected. Pieces about 1 mm wide were used for incubations. The incubations were performed in stoppered Eppendorf tubes at 37°C in a 5% CO_2-95% O_2 atmosphere. After a 60 min preincubation period, the septum was incubated for four 15-min periods in basal or stimulating media in a final volume of 150 µl. The amount of secreted TRH was determined by RIA.

Immunoneutralization of endogenous TRH with specific antibody results in a deeper decrease of mean arterial pressure (to 22.2 ± 3.7 and 40 ± 10.6 mmHg in experimental and control rats, respectively, $p<0.05$, n=6, Student's t test) at the end of bleeding of experimental rats. RT PCR revealed two times higher TRH expression in LA than in LV of intact rats. Slices secreted measurable amount of TRH. Angiotensin II (10 nM) added into the medium significantly decreased basal secretion of TRH by 38% (pairwise multiple comparison procedures (Tukey test): $p<0.001$), and this effect was prevented by addition of Losartan, an inhibitor of AT1 receptors. Hyposmotic medium (202 mOsm) or high KCl significantly ($p<0.05$) increased the amount of secreted TRH. The effect of hyposmotic stimulation could not be inhibited by angiotensin II (10 or 100 nM).

In conclusion, endogenous TRH has a role in regulation of blood pressure in bleeding rats. TRH secretion from heart slices possesses attributes of regulated secretion: it could be either stimulated or inhibited. Angiotensin II inhibits TRH secretion by heart tissue and its effect is mediated by AT1 receptors.

Garcia SI et al.(2001). Hypertension 37, 365-370.

Jin H et al. (2004). Circulation 109, 2240-2245

This work was supported by project SP 51/0280800/0280802, project 23191/23 VEGA, project 017/2001 - US Slovak Science and Technology Program and project APVT-51-016002.

Where applicable, the experiments described here conform with Physiological Society ethical requirements.

PC8

HERG channel blockade by two antibiotics, erythromycin and moxifloxacin: resistance to mutation of the S6 residues F656 and Y652

R.S. Duncan[1], J.M. Ridley[1], J.T. Milnes[1], D.J. Leishman[2], J.C. Hancox[1] and H.J. Witchel[1]

[1]Dept of Physiology, University of Bristol, Bristol, UK and [2]Ion Channel Pharmacology Group, Pfizer Global Research and Development, Sandwich, UK

The effects of two antibiotics, moxifloxacin, a fluoroquinolone, and erythromycin, a macrolide, on the HERG (human *ether-a-go-go* related gene) potassium channel were explored. Both of these antibiotics are known to have QT prolonging effects on the human ECG (Demolis *et al.* 2000; Mishra *et al.* 1999). The effects of these two drugs on both wild type and mutant heterologous HERG potassium currents (I_{HERG}) expressed in HEK or CHO cell lines were assessed using 'whole-cell' patch-clamp. Experiments were superfused at 37°C unless otherwise stated. Results are mean ± S.E.M.

Both moxifloxacin and erythromycin blocked HERG in a concentration dependent manner. IC_{50}s were 54.9µM (n=5 for each of four drug concentrations) and 72.8µM (n=5 for each of 4 drug concentrations) for erythromycin and moxifloxacin, respectively. The time dependence of erythromycin block was further characterised. Cells were held at -100 mV and then subjected to a 'short depolarisation' (+40 mV for 10 ms). I_{HERG} tails were then observed at -40 mV (Milnes *et al.* 2003). Upon application of 60µM erythromycin, we observed 25 ± 6% block (n=5). The depolarisation was then lengthened to 200ms and 54 ± 3% block was seen (n=5, paired t test, $P<0.01$). These results are concordant with erythromycin either producing a rapid open-state-dependent block, or that the block includes a component of both open-state-dependent and closed-state-dependent block.

Block by erythromycin was found to be strongly temperature dependent; 60µM erythromycin produced a block of 15 ± 9% (n=7) at 22°C compared to 51 ± 2% at 37°C (n=5, unpaired t test, $P=<0.0001$). Kirsch *et al.* (2004) found a similar temperature dependence for HERG blockade by erythromycin and suggested the reduction in block at room temperature could be due to the drug being much slower to cross the membrane and to access its binding site.

The canonical HERG drug-binding site is thought to be located in the S6 domain. Two amino acid residues, F656 and Y652, are key constituents of this high affinity drug-binding site. Mutation of these residues to alanine only partially attenuated the HERG block by either moxifloxacin or erythromycin. These results provide further evidence for the existence of a second HERG drug-binding site distinct from the canonical S6 site.

Demolis J et al. (2000). *Clinical Pharmacology and Therapeutics* **68**, 658-666.

Kirsch GE et al. (2004). *J Pharmacol Toxicol Methods* **50**, 93-101.

Milnes JT et al. (2003). *FEBS Lett* **547**, 20-26

Mishra A et al. (1999). *Chest* **115**, 983-986.

Where applicable, the experiments described here conform with Physiological Society ethical requirements.

PC9

PPAR-mediated regulation of cardiac lipid metabolism is not impaired in hypertrophic neonatal cardiac myocytes

G.J. van der Vusse, A. Gilde, P. Smeets, P. Willemsen and M. van Bilsen

Physiology, Cardiovascular Research Institute Maastricht, Maastricht, Netherlands

The currently accepted paradigm is that fatty acid (FA) metabolism is attenuated in the hypertrophied and failing heart. This is thought to be due to a decreased expression of genes involved in FA uptake and metabolism, secondary to a decline in peroxisome proliferator-activated receptor α (PPARα) activity. The aim of the present study was to investigate the relation between the expression of FA handling genes and FA oxidation rate during cardiac hypertrophy using neonatal rat cardiomyocytes (NCM) from humanely killed neonatal rats as a model system. Therefore, NCM were exposed to the α1-adrenergic agonist phenylephrine (PE, 10^{-5} M) or thyroid hormone (T3, 10^{-8} M) in the absence or presence of natural (FA) or synthetic (Wy-14,643) PPARα ligands for 48 h. Experiments were performed

at least in triplicate. Statistical analysis of group differences was performed with one-way ANOVA, followed by two-tailed Student's t test.
PE and T3 stimuli induced distinct cellular phenotypes as was evident from cell morphology and the differential expression of the hypertrophic marker gene atrial natriuretic factor and sarcoplasmic reticulum Ca^{2+}-ATPase 2a. PE and T3 affected neither basal expression nor PPAR-mediated induction of a panel of lipid metabolising genes at the mRNA or protein level. In transient transfection studies the basal activity of the human muscle-type carnitine palmitoyl transferase-I promoter was not affected by PE or T3. PE, but not T3, markedly increased the oxidation of [^{14}C]-palmitate from 0.15±0.04 to 0.45±0.16 nmol palmitate mg^{-1} min^{-1} ($p<0.05$), whereas the oxidation rates of glucose (0.70±0.09 nmol glucose mg^{-1} min^{-1}) and pyruvate (0.50±0.10 nmol pyruvate mg^{-1} min^{-1}) remained constant. The PPAR-mediated increase in [^{14}C]-palmitate oxidation rate was not affected by PE or T3. The present findings point to a selective increase of FA oxidation capacity in PE-stimulated hypertrophied cardiomyocytes independent of changes in the expression of FA handling genes, thereby challenging the current paradigm that cardiac hypertrophy is associated with a decline in PPARα activity and, consequently, impaired fatty acid metabolism.

Supported by Netherlands Heart Foundation grant 1998T015.

Where applicable, the experiments described here conform with Physiological Society ethical requirements.

PC10

Stabilization of re-entry in canine virtual ventricles by decreasing the slow inward Ca^{2+} current

O.V. Aslanidi[1], E.W. Hsu[2] and A.V. Holden[1]

[1]School of Biomedical Sciences & Cardiovascular Research Institute, University of Leeds, Leeds, UK and [2]Department of Biomedical Engineering, Duke University, Durham, NC, USA

Ventricular fibrillation (VF) is believed to arise by the breakdown of re-entrant scroll waves of excitation. We use a computational model of re-entry and development of VF in a family of homogenous anisotropic canine ventricular architectures that have been algorithmically reconstructed from diffusion tensor magnetic resonance imaging (DT-MRI) datasets (Benson *et al.* 2005). The model is a monodomain reaction-diffusion system with the Fenton-Karma MBR excitation kinetics (Fenton & Karma, 1998: see Table 1) and anisotropic diffusion within the DT-MRI derived 3D ventricular anatomy. A single re-entrant scroll wave is initiated in the left ventricular free wall (Clayton & Holden, 2004). For the standard parameter set, the scroll breaks down after about 500 ms, evolving into VF. The single filament of the scroll wave (*i.e.*, a phase singularity around which the wave rotates) undergoes a cascade of splittings, which leads to the emergence of multiple irregularly moving filaments. For decreased slow inward Ca^{2+} current, and hence shorter cellular action potential duration (APD), the scroll is apparently stable (Figure 1), and persists for 3 s. A re-entrant spiral wave initiated in an isotropic 2D tissue is stable for both normal and decreased Ca^{2+} current. The breakdown of a re-entrant wave in a homogeneous anisotropic tissue can be due to either cellular restitution properties (Garfinkel *et al.* 2000), or the tissue anisotropy (Fenton & Karma, 1998): our results demonstrate that breakdown due to anisotropy can be prevented by changing excitation parameters that decrease APD and flatten the restitution curve.

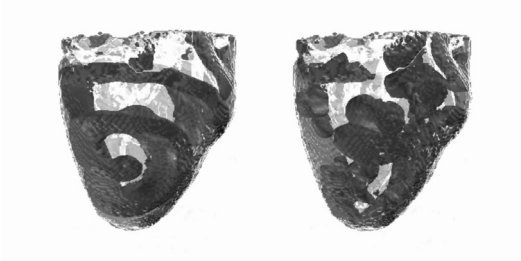

Figure 1. Re-entry and VF in the DT-MRI virtual ventricles. Snapshots of dark-grey voltage isosurfaces are shown within the pale-grey ventricles at 2 s. The slow inward Ca2+ current is either normal (right) or decreased by 50% (left), whereas the tissue anisotropy is the same in both cases.

Benson AP *et al.* (2005). *This Proceedings* .

Fenton F & Karma A (1998). *Chaos* **8**, 20-47.

Clayton RH & Holden AV (2004). *IEEE Trans Biomed Eng* **51**, 28-34.

Garfinkel A *et al.* (2000). *Proc Natl Acad Sci USA* **97**, 6061-66.

This research was funded by the MRC and EPSRC UK, and the European Network of Excellence 'BioSim'.

Where applicable, the experiments described here conform with Physiological Society ethical requirements.

PC11

Reconstruction and visualisation of cardiac ventricular geometry and architecture from diffusion tensor magnetic resonance imaging

A.P. Benson[1], P. Li[1], E.W. Hsu[2] and A.V. Holden[1]

[1]Computational Biology Laboratory, School of Biomedical Sciences, University of Leeds, Leeds, UK and [2]Department of Biomedical Engineering, Duke University, Durham, NC, USA

We reconstruct and visualise cardiac geometry and fibre architecture of post mortem canine hearts from diffusion tensor magnetic resonance imaging (DT-MRI) data sets. DT-MRI calculates 3 eigenvalues and 3 eigenvectors for the diffusion tensor for protons at each pixel throughout 3-dimensional tissue. The eigenvalues can be used to calculate a normalised measure of anisotropy: the primary eigenvector provides a measure of fibre orientation, while the tertiary eigenvector provides an index of sheet structure and orthotropy (Hsu *et al.* 1998).
We visualise these DT-MRI tensors and extract the fibre orientation throughout the ventricles from the primary eigenvalues, or a combination of the linear and planar components of the tensor, with the 3D geometry of the ventricles reconstructed by stacking DT-MRI data slices. Fibre orientation in the left ventricular free wall, given by the helix angle of the primary eigenvector, changes smoothly from approximately −60 deg at the epicardial surface to 70 deg at the endocardial surface (Figure 1A). The image matrix for the canine ventricular data is $256 \times 128 \times 128$, representing a physical field of view of $100 \times 100 \times 76.8$ mm;

each pixel in the DT-MRI data slices is 780 μm square, sufficient to visualise the boundaries of the papillary muscles and their insertions (Figure 1B), which are blurred by the temporal averaging of *in vivo* MRI of the beating heart.
All stages of the model construction have been algorithmically automated: hence, DT-MRI of isolated hearts provides a high throughput method of reconstruction of detailed ventricular geometry and architecture that can be used for the computation of electrophysiology (Aslanidi *et al.* 2005).

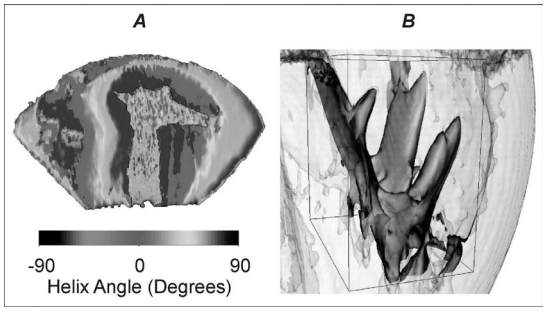

Figure 1. A, 3-dimensional reconstruction of a section of canine left ventricle showing a smooth transmural change in the helix angle of the primary eigenvector, an indicator of fibre orientation. B, the resolution of the DT-MRI data sets is sufficient to allow visualisation of papillary muscle.

Aslanidi OV *et al.* (2005). (this proceedings volume).

Hsu EW *et al.* (1998). *Am J Physiol* **274**, H1627-34.

APB is supported by a Medical Research Council bio-informatics (computational biology) priority area research studentship (G74/63).

Where applicable, the experiments described here conform with Physiological Society ethical requirements.

PC12

Action potential duration, conduction velocity restitution, and vulnerability to re-entry in a computational model of human failing heart tissue

S. Kharche[1], H. Zhang[2] and A.V. Holden[1]

[1]Biomedical Sciences, University of Leeds, Leeds, UK and [2]Biological Physics Group, Department of Physics, UMIST, Manchester

Ventricular failure is associated with remodelling of ion channels and intracellular Ca^{2+} dynamics. A model (Preibe & Beuckelmann, 1998) for normal and failing (remodelled I_{K1}, I_{NaCa}, I_{NaK}, Ca^{2+}-ATPase of the SR) heart cells was incorporated into a partial differential equation (PDE) tissue model to determine how the remodelling associated with heart failure can alter propagation patterns. We use the simple Euler method to integrate the PDE with a time step of 0.02 ms and a space step of 0.2 mm with a diffusion constant, D = 0.154 mm^2/ms.
Dynamic action potential duration (APD) restitution was obtained by pre-pacing the cell models 40 times to obtain the final diastolic interval (DI) and APD. Conduction velocity (CV) restitution was obtained by pacing the 1D spatial models for 5 s at a frequency of 1 Hz. CV of a 6th premature propagating wave was measured. Vulnerable window (VW) (Biktashev *et al.* 1998) in 1D was measured.
The dynamic restitution curve for the failing case has a region of negative slope at high stimulation rate (small period) while is positive in the control case. The maximal magnitude of the slopes of both curves is < 1 and both the normal and failing models show alternans. At fast pacing rates electrical alternans were observed for a basic cycle length (BCL) of < 392 ms in control cell, and for BCL of < 665 ms in the failing cell.
The CV for a solitary wave in the failing case is marginally greater than in the non-failing case (7%). The CV restitution is shifted upward in failing tissue. The measured vulnerable window (VW) for the tissue to re-entry is 5 ms for the control and 7 ms for the failing case. Heart failure increased vulnerability of the tissue to re-entry by 40% and shifted the timing of the window significantly.
In conclusion, heart failure induced remodelling ion channel kinetics and intracellular Ca^{2+} handling has a significant impact on the rate dependent electrical action potential and conduction properties of excitation waves. It also increases vulnerability of the tissue to arrhythmogenesis.

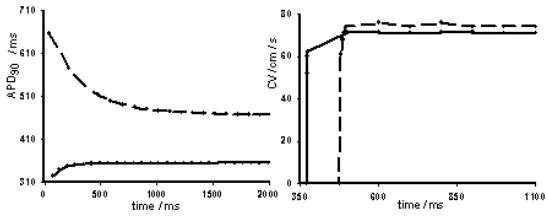

Figure 1. Restitution properties for normal (solid dotted lines) and for failure (dash dotted lines) cell and tissue models. Left panel shows dynamic APD restitution for cell and right panel shows CV restitution curve for 1D tissue.

Figure 1. Restitution properties for normal (continuous dotted lines) and for failure (dash dotted lines) cell and tissue models. Left panel shows dynamic APD restitution for cell and right panel shows CV restitution curve for 1D tissue.

Priebe L & Beuckelmann DJ (1998). Circ Res **82**, 1206-1223.

Biktashev VN & Holden AV (1998). Chaos **8**, 48-56.

This work was supported by EU BioSim (contract 005137), the British Heart Foundation, and EPSRC (GR1R92592/01).

Where applicable, the experiments described here conform with Physiological Society ethical requirements.

PC13

Abolition of G-protein inhibitory subunit signalling does not reveal a positive inotropic effect of microtubule disruption in rat ventricular myocytes

A.D. O'Connell, S.C. Calaghan and E. White

School of Biomedical Sciences, Universiy of Leeds, Leeds, UK

In neuronal tissue, free tubulin can activate both stimulatory (Gs) and inhibitory (Gi) G-protein α-subunits via transfer of GTP from the exchangeable GTP-binding site on β-tubulin (Rasenick *et al.* 1981). It is debatable whether such signalling occurs in the heart. Colchicine-induced microtubule disruption, which increases free tubulin, is reported

to be without effect on shortening or $[Ca^{2+}]_i$ transient amplitude in normal rat ventricular myocytes (Calaghan *et al.* 2001, 2004). In contrast, Kerfant *et al.* (2001) have shown an increase in $[Ca^{2+}]_i$ transient amplitude after colchicine treatment in the same preparation. These workers suggested that Gs α-subunit stimulation of adenyl cyclase underlies increased $[Ca^{2+}]_i$ transients after microtubule disruption. In this study we determine whether a predominance of the Gi pathway in our animal model is masking Gs responses that might increase contraction or $[Ca^{2+}]_i$ transients after colchicine treatment.

Male Wistar rats were killed humanely, and myocytes were isolated enzymatically from the right ventricle. Cells were incubated in 1.5 mg ml^{-1} pertussis toxin (PTX, a Gi α-subunit inhibitor) and/or 10 μM colchicine for at least 1.5 h in normal Tyrode solution at room temperature. Shortening (determined by video-edge detection) and $[Ca^{2+}]_i$ transients were measured simultaneously in fura-2-loaded cells (37 °C, 1 Hz stimulation). Statistical analysis was performed using one-way ANOVA.

The effect of colchicine and PTX on shortening and $[Ca^{2+}]_i$ transient amplitude is shown in Fig. 1. Treatment with colchicine or PTX alone did not alter the shortening amplitude or the $[Ca^{2+}]_i$ transient when compared with controls ($P>0.05$). Furthermore, co-incubation with PTX did not change the shortening or $[Ca^{2+}]_i$ transient response to colchicine ($P>0.05$).

PTX has no effect on shortening or $[Ca^{2+}]_i$ transient characteristics nor does it modulate the response to colchicine. We conclude, therefore, that predominant Gi α-subunit signalling cannot explain the lack of effect of colchicine on contraction or $[Ca^{2+}]_i$ transients under the conditions of our experiments. Our data are in agreement with a body of evidence showing that microtubule disruption by colchicine in the healthy cardiac cell is without functional consequences.

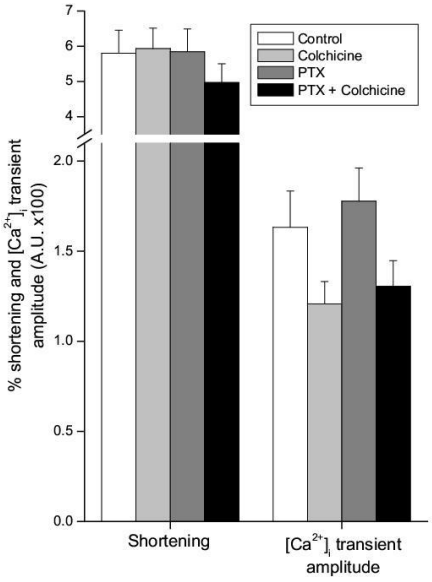

Figure 1: The effect of PTX and/or colchicine on shortening (as a % resting cell length) and intracellular calcium transient amplitude in rat ventricular myocytes. Bars are means +SEM (n=36-41).

Calaghan SC, Le Guennec JY & White E (2001). *Circ Res* **88**, E32-E37.

Calaghan SC, Le Guennec JY & White E (2004). *Prog Biophys Mol Biol* **84**, 29-59.

Kerfant BG, Vassort G & Gomez AM (2001). *Circ Res* **88**, E59-E65.

Rasenick MM, Stein PJ & Bitensky MW (1981). *Nature* **294**, 560-562.

This work is supported by the BHF.

Where applicable, the experiments described here conform with Physiological Society ethical requirements.

PC14

Reentry initiated by spontaneous early afterdepolarizations in a ventricular virtual tissue

W. Tong[1], R.H. Clayton[2] and A.V. Holden[1]

[1]Computational Biology Laboratory, University of Leeds, Leeds, UK and [2]Department of Computer Science, University of Sheffield, Sheffield, UK

One hypothesis for arrhythmogenesis is that a spontaneous ectopic excitation occurring during the vulnerable window of a propagating wave can initiate reentry. This has been demonstrated experimentally and computationally with artificial initiation methods (Starmer *et al.* 1993; Clayton & Holden, 2002) but spontaneous onset of reentry is rarely observed. The ectopic events that leads to early afterdepolarizations (EADs) in single cells, unidirectional propagations in 1-D fibre, reentrant spiral waves in 2-D tissue and rotors and scroll rings in 3-D slabs, could be the result of stochastic perturbations amplified in tissue regions that are near to bifurcation points. Therefore, a deterministic Luo-Rudy ventricular tissue (Faber & Rudy, 2000) was stochastically perturbed to determine the probability and conditions for spontaneous initiation of an ectopic beat and reentry (Clayton *et al.* 2003).

EADs can be caused by low current density of the fast and slow delayed rectifying K^+ currents (I_{Kr}, I_{Ks}), and incomplete inactivation of fast Na^+ current. M cells, with the least I_{Ks} density, following a long diastolic interval are most prone to EADs. Therefore, the maximum conductance of I_{Ks} (g_{Ks}) of a M cell was reduced to 83% of the standard value, just below the critical point of producing an EAD. Addition of a small noise current at this critical g_{Ks} can trigger or reduce EADs in a single cell (Figure 1A). However, this bifurcation point is sensitive to $[Na^+]_i$: high $[Na^+]_i$ will push the critical g_{Ks} to a lower level.

In a homogenous 1-D tissue, the critical level of g_{Ks} is further reduced due to the electronic spread of membrane potential. The propagating wave develops ectopics as g_{Ks} is reduced to 74.8%. An ectopic can be a localised EAD or a bi-directional source, i.e. a focus. With g_{Ks} at 74.815%, a small noise current (± 0.1 $mAcm^{-2}$) evokes unidirectional propagations: (1) antegrade, equivalent to an ectopic; (2) retrograde, equivalent to a reentrant source.

Fluctuations in membrane potential triggered ectopics can initiate reentry. However, such potentially reentrant activity occurred with a low probability (3 out of 71 cases), and was confined in a narrow range within the parameter space (0.03%) (Fig. 1B).

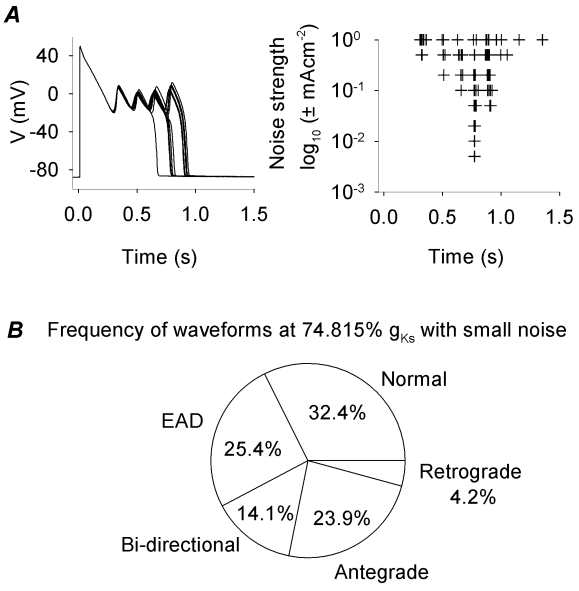

Figure 1. A, fffect of noise levels (± 0.005 to 1 $mAcm^{-2}$) on action potentials (APs) for M cells at 83% g_Ks. Each combination is repeated 20 times. Left, superimposed APs with noise at ± 0.1 $mAcm^{-2}$; right, action potential durations of all cases. B, frequencies of different propagations with 74.815% g_Ks and noise (± 0.1 $mAcm^{-2}$).

Starmer CF *et al.* (1993). *Biophys J* **65**, 1775-1787.

Clayton RH & Holden AV (2002). *Int J Bioelectromag* **2**

Clayton RH *et al.* (2003). *Int J Bif Chaos* **13**, 3835-3843.

Faber GM & Rudy Y (2000). *Biophys J* **78**, 2392-404.

Supported by the EU Network of Excellence 'BioSim' (005137) and a BHF research studentship (FS/03/075/15914).

Where applicable, the experiments described here conform with Physiological Society ethical requirements.

PC15

Cysteine protects isolated rat cardiomyocytes during oxidative stress by increasing the activity of glutathione peroxidase

A. Hall[2], C. Naim[3], S. Tavassoli[2], B. Shukla[1], M. El Zouhairi[3], M. Suleiman[1] and N. King[1]

[1]Clinical Science @ South Bristol, University of Bristol, Bristol, UK, [2]Physiology, University of Bristol, Bristol, UK and [3]University of Balamand, Beirut, Lebanon

The uncontrolled generation of reactive oxygen species is a major cause of ischaemia-reperfusion injury (Dhalla *et al.* 2000). We have previously shown that the sulphydryl containing amino acid cysteine is protective against ischaemia reperfusion in whole heart (Schackebaei *et al.* 2004) and against oxidative stress in isolated cardiomyocytes (Evans *et al.* 2004). However, the mechanisms underlying the protective effects of cysteine remain unclear. The aim of this study was to test the hypothesis that cysteine increases activity of glutathione peroxidase (GPx).

Male Wistar rats were humanely killed and ventricular myocytes isolated as described previously (King *et al.* 2003). Cells were incubated with or without (control) 0.5mM L-cysteine for 2 h at room temperature. Myocytes were then placed in suspension on the stage of a microscope at 37°C and stimulated at 0.2Hz. They were exposed to oxidative stress by superfusion with a Tyrode solution containing 0.2mM H_2O_2. Measurements were taken of the time to hypercontracture. In a separate series of experiments GPx was extracted, isolated and quantified as described previously (King *et al.* 2003).

Incubation with cysteine significantly increased time to hypercontracture during oxidative stress (control 885±51.2 s vs. cysteine incubation 1108±0.234 s, $p<0.001$ (unpaired t test), n=4, mean±SEM). Additionally, the activity of the enzyme GPx was significantly greater in the cysteine incubated cells (1.108±0.234 mU/mg protein) compared to the control cells (0.538±0.1 mU/mg protein, $p<0.05$ (unpaired t test), n =4-5, mean±SEM). These results provide further evidence that incubation with 0.5mM cysteine protects against oxidative stress in isolated cardiomyocytes and that this may be as a result of stimulated GPx activity.

Dhalla NS *et al.* (2000). *Cardiovasc Res* **47**, 448-456.

Evans E*et al.* (2004). *J Physiol* **557P**, 17PC.

King N *et al.* (2003). *J Mol Cell Cardiol***35**, 975-984.

Shackebaei D *et al.* (2004). *J Physiol* **557P**, 16PC.

Supported by the BHF.

Where applicable, the experiments described here conform with Physiological Society ethical requirements.

PC16

The effects of carbenoxolone and octanol on action potential characteristics in guinea-pig left ventricular myocardium

P. Dhillon[2], R. Gray[1], N. Peters[2] and C.H. Fry[1]

[1]Institute of Urology, University College London, London, UK and [2]Cardiac Electrophysiology Group, Imperial College London, London, UK

Alterations to cardiac gap-junction coupling and consequent changes to action potential (AP) propagation may predispose the heart to arrhythmias. Known cellular uncoupling agents may also alter membrane ionic currents and hence AP parameters, complicating studies of the their action. We aimed to compare the effects of carbenoxolone and *n*-octanol on AP morphology and conduction velocity (θ) in guinea-pig left ventricular myocardium.

Male Dunkin-Hartley guinea pigs were sacrificed after schedule 1 methods, the heart was removed and left ventricular papillary muscles superfused in Tyrodes solution at 37 C. Longitudinal θ and AP parameters were measured before, during and after addition of either 20μM carbenoxolone or octanol 0.096ml/ml in Tyrodes solution for up to 60 minutes. Data are mean ±SD, and sets were compared with Students t-test, significance at $p<0.05$. 20μM carbenoxolone had no effect on AP parameters (control first): i) action potential duration at 50% repolarisation, APD_{50}; 154±12 vs 155±16 ms, n=6: ii) APD_{95}; 193±17 vs 205±17 ms, n=6: iii) maximum AP upstroke velocity, V_{max}; 215.9±44.9 vs 195.6±46.2 V/s, n=6: iv) the time constant of the AP foot, τ_{ap},;

0.28±0.04 vs 0.28±0.02 ms, n=5. However, carbenoxolone significantly slowed θ, from 76.5±5.3 to 39.8±5.2 cm.s-1 (n=5) after 45 minutes. R_i, derived from the cable equation $\theta^2 = a/2R_i.C_m.\tau_{ap}$ (a is cell radius, and C_m = 1 μF/cm^2) increased from 395±28 to 1528±314 Ω.cm. The effects of carbenoxolone were irreversible at this concentration.

n-Octanol also significantly slowed θ by 29.6±14.9% (n=5) after 7 minutes, and further by 65.8±26.8% (n=3) after 30 minutes. Conduction was completely blocked within 10 minutes in two of five preparations. APD_{50} decreased from 163±15 to 101±16 ms (n=5) after 7 minutes and to 96±15 ms (n=3) after 30 minutes. APD_{95} decreased from 209±11 to 141±18 ms after 3 minutes, and to 127±14 ms after 30 minutes. V_{max} and τ_{ap} were unaffected. After superfusion with Tyrodes for 60 minutes θ and AP parameters returned to normal in all preparations.

Carbenoxolone slowed ventricular AP conduction by increasing R_i, and without altering AP morphology, whereas *n*-octanol also significantly reduced APD. These results suggest that carbenoxolone, but not *n*-octanol, specifically uncouples gap-junctions without effect on ionic currents.

We thank the British Heart Foundation for financial assistance

Where applicable, the experiments described here conform with Physiological Society ethical requirements.

PC17

Morphological and contractile characteristics of myocytes isolated from apolipoprotein E knockout mouse heart

A. Chase, C.L. Jackson, G.D. Angelini and M. Suleiman

Bristol Heart Institute, University of Bristol, Bristol, UK

Deletions of the genes for apolipoprotein E (ApoE$^{-/-}$) result in severe atherosclerosis, with the formation of lesions strikingly similar to those found in humans (Breslow 1996; Johnson & Jackson, 2001). ApoE$^{-/-}$ mice fed on a high fat diet show lesions in the coronaries and evidence of myocardial infarction (Williams et al. 2002). Nothing is known about the characteristics of the myocytes in these diseased hearts. The aim of this work was to isolate myocytes from ApoE$^{-/-}$ (fed on high fat diet) and their strain-matched, age-matched wild-type (fed on normal chow) mice and to compare their morphology and contractile properties.

ApoE$^{-/-}$ mice (7-8 months old) fed on a high fat diet for 5-6 months and their matched wild-type mice were humanely killed, and the hearts were removed and perfused in the Langendorff mode. Myocytes were enzymatically isolated as described previously (Williams et al. 2001). Isolated myocytes were perfused with Tyrode solution and field stimulated at different frequencies at 37°C. Cell length measurements were made using an edge detector. All results are expressed as mean ± S.E.M. and analysed using an unpaired t test.

Myocytes from ApoE$^{-/-}$ mice were significantly ($p<0.05$) shorter in length and width than wild-type mice (112±3 vs. 142±5 μm in length and 23.9±0.9 vs. 28.8±1.6 μm in width, n=30-70 myocytes isolated from 6 hearts from each group). When myocytes were stimulated at 0.2 Hz, there was no difference in the amplitude of contraction (% of cell length): 12.7±1.3 vs. 13.5±0.8%, for ApoE$^{-/-}$ and wild-type mice, respectively). However, upon increasing the rate of stimulation there was a significant decrease in the amplitude of contraction in ApoE$^{-/-}$ but not in wild-type myocytes (Fig. 1). Furthermore, at higher frequencies, the diastolic length of the myocytes decreased in ApoE$^{-/-}$ but not in wild-type.

In conclusion, this work shows that myocytes of ischaemically diseased hearts have different characteristics from wild-type. Further investigation is required to ascertain whether myocytes from ApoE-/- mice fed on chow diet (control) display similar characteristics. This work may have clinical implications for patients with coronary heart disease.

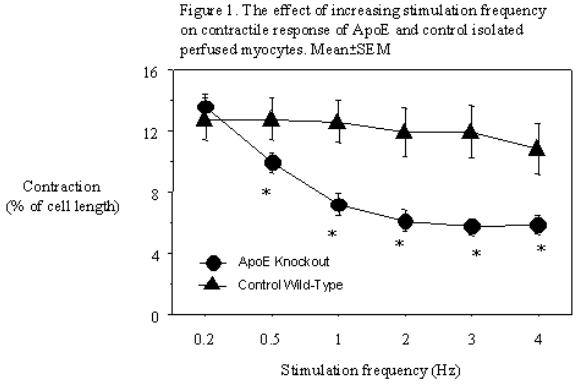

Figure 1.

Breslow JL (1996). Science 272, 685-688.

Johnson JL & Jackson CL (2001). Atherosclerosis 154, 399-406.

Williams H et al. (2002). Arterioscler Thromb Vasc Biol 22, 788-792.

Williams H et al. (2001). J Mol Cell Cardiol 33, 2109-2119.

This work is supported by the British Heart Foundation.

Where applicable, the experiments described here conform with Physiological Society ethical requirements.

PC18

The effect of metabolic inhibition on myocytes isolated from apolipoprotein E knockout mouse heart

A. Chase, H. Lin, C.L. Jackson, G.D. Angelini and M. Suleiman

Bristol Heart Institute, University of Bristol, Bristol, UK

Deletion of the gene for apolipoprotein E (ApoE$^{-/-}$) results in severe atherosclerosis in mice, with the formation of lesions strikingly similar to those found in humans (Breslow 1996; Johnson & Jackson 2001). ApoE$^{-/-}$ mice fed on high fat diet show lesions in the coronaries and evidence of myocardial infarction (Williams et al. 2002). Nothing is known about the vulnerability of the myocytes in these diseased hearts to cardiac insults. The aim of this work was to isolate myocytes from ApoE$^{-/-}$ mice (fed on high fat diet) and their strain-matched, age-matched wild-type (fed normal chow diet) and to compare their morphological and contractile properties during metabolic inhibition.

ApoE$^{-/-}$ mice (7-8 months old) fed on high fat diet for 5-6 months and their matched wild-type were humanely killed, and the hearts were removed and perfused in the Langendorff mode. Myocytes were enzymatically isolated as described previously (Williams

H. et al. 2001). Isolated myocytes were perfused with normal Tyrode solution and field stimulated at 0.2 Hz at 37°C. For metabolic inhibition, myocytes were exposed to glucose-free solution containing 2.5mmol/L sodium cyanide. Myocytes were monitored for their changes in shape and contractile activity. All results are expressed as mean ±S.E.M. and analysed using an unpaired t test.

Following exposure to glucose-free cyanide containing Tyrode solution, myocytes gradually cease beating and enter a state of rigor. These changes occurred at a significantly ($p<0.05$, n=32 myocytes) faster rate in myocytes from $ApoE^{-/-}$ in comparison to wild-type (16.1±0.8 vs. 25.4±1.0 min for cessation of contractile activity and 19.3±0.9 vs. 29.6±1.1 min for rigor contracture). Upon reperfusion with normal Tyrode, the extent of contractile recovery was dependent on the duration of time in rigor. After long duration in rigor (30-40 min) none of the $ApoE^{-/-}$ myocytes recovered whereas 80% of wild-type myocytes displayed contractile recovery. In order to assess the viability of the myocytes, the dye trypan blue was used. Preliminary data showed that more wild-type myocytes were able to exclude the dye following long periods of cyanide exposure than $ApoE^{-/-}$ myocytes. In conclusion, this work shows that myocytes of ischaemically diseased hearts are more vulnerable to metabolic inhibition than wild-type myocytes. Differences in metabolism and ionic mobilization may explain these observations. Whether these observations occur in myocytes of $ApoE^{-/-}$ mice fed on normal chow diet requires further investigation.

Breslow JL (1996). Science 272, 685-688.

Johnson JL & Jackson CL (2001). Atherosclerosis 154, 399-406.

Williams H et al. (2002). Arterioscler Thromb Vasc Biol 22, 788-792.

Williams H et al. (2001). J Mol Cell Cardiol 33, 2109-2119.

This work is supported by the British Heart Foundation.

Where applicable, the experiments described here conform with Physiological Society ethical requirements.

PC19

Age-related differences in rat cardiac interleukin-6: implications for vulnerability to reperfusion injury

E.K. Moore[2], A. Chase[1], H. Lin[1], N. King[1] and M. Suleiman[1]

[1]Bristol Heart Institute, University of Bristol, Bristol, UK and [2]Department of Physiology, University of Bristol, Bristol, UK

The pro-inflammatory cytokine interleukin-6 (IL-6) has been implicated in tissue (e.g. cardiac and lung) damage following ischaemia and reperfusion (Benson et al. 2003; Chiang et al. 2001; Teng et al. 2004). Whether this increase contributes to injury or is a consequence of injury remains unresolved. The vulnerability of the myocardium to ischaemia and reperfusion changes during development (Ostadal et al. 1999). For example, we have shown that the extent of reperfusion damage changes during different stages of development with 14 day old hearts showing more resistance compared with 7 and 21 day old hearts (Modi & Suleiman, 2004). In the present study we investigated whether these differences are related to the basal level of myocardial IL-6 in different age groups.

Male wistar rats (7, 14, 21 and 28 days old) were humanely killed, and the hearts were removed and rinsed in ice-cold buffer. Ventricular cardiac tissue was snap frozen in liquid nitrogen and processed for determination of total protein content and IL-6 content. Enzyme-linked immunosorbent assay was used to measure the concentration of IL-6 protein in heart tissue. All results are expressed means ± S.E.M. and analysed using ANOVA with Fischer's PLSD post hoc test.

Figure 1 shows that the concentration of IL-6 in rat hearts changes during different stages of development. IL-6 levels were lowest in 7 day old hearts but increased with age reaching maximum at 21 days. Whether these differences in the basal level of IL6 contribute to protection against reperfusion injury during development requires further investigation.

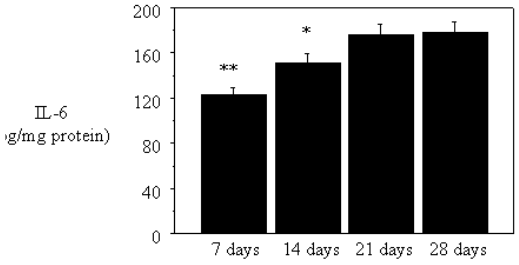

Figure 1. Changes in the myocardial concentration of IL-6 during developmer Mean ±SEM (n=3-5). * vs. 28 days. **vs. 21 and 28 days, P<0.05.

Figure 1.

Benson S. et al. (2003). J Physiol 552P, P32.

Chiang CH et al. (2001). Clinical Science 101, 285-294.

Teng S et al. (2004). Am J Physiol 286, L137-L142.

Ostadal B et al. (1999). Physiol Rev 79, 635-659.

Modi P & Suleiman MS (2004). Amino Acids 26, 65-70.

Where applicable, the experiments described here conform with Physiological Society ethical requirements.

PC20

Pyruvate is cardioprotective in a model of Langendorff perfused immature rat heart

I.H. Khan[1], N. King[1], A.P. Halestrap[2], G.D. Angelini[1] and M. Suleiman[1]

[1]Bristol Heart Institute, University of Bristol, Bristol, UK and [2]Department of Biochemistry, University of Bristol, Bristol, UK

Immature (14 days old) rat heart is more resistant to cardiac ischaemia and reperfusion than adult heart (Modi & Suleiman 2004). The reason for this difference is not known although developmental changes including intracellular calcium mobilisation and metabolism have been implicated. We have shown that the intermediary metabolite pyruvate attenuates ischaemia/reperfusion injury in rat adult heart (Kerr et al. 1999). Whether pyruvate is also cardioprotective in the more resistant immature rat heart is not currently known.

Male Wistar rats (14 days old) were humanely killed, and the hearts were quickly removed, cannulated in the Langendorff mode and perfused with Krebs buffer at 37°C as described previously (Modi & Suleiman 2004). After 20 min equilibration,

control hearts (n=4) were exposed to normothermic global ischaemia for 60 minutes. Hearts were then reperfused for 50 min and functional recovery determined. In the experimental group (n=8), 10 mmol/l pyruvate was present 10 min before and during ischaemia, but was washed out after 20 min reperfusion. Left ventricular developed pressure (and computed heart rate) was measured using a balloon inserted in the left ventricle. All results are expressed means ± S.E.M. and analysed using ANOVA with Fischer's PLSD post hoc test.

Pyruvate had no effect on heart rate but slightly increased LVDP (39.7 ± 5 to 44.0 ±5 mmHg). Time to induce contractile arrest was similar for both groups (5.2 ± 0.8 vs. 4.4 ± 0.5min for pyruvate and control, respectively). Pyruvate significantly increased the time to onset of ischaemic contracture (17.4 ± 0.8 vs. 7.8 ± 1.1min, $p<0.05$). Figure 1 shows that pyruvate significantly ($p<0.05$) improved % recovery in rate pressure product (mmHg. beats min^{-1}) as measured at the end of reperfusion.

Our data demonstrate that pyruvate is cardioprotective in the immature heart just as it is in the adult heart. The delay in the onset of ischaemic contracture may underlie its cardioprotective action. However, whether the mechanism is similar to adult heart remains to be investigated.

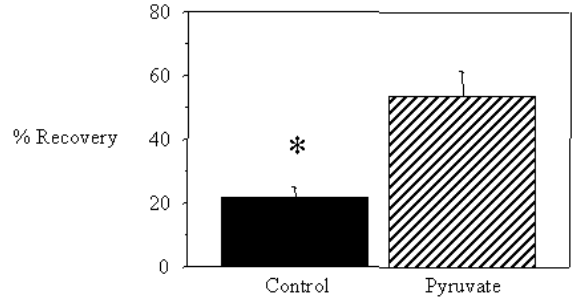

Figure 1. Percentage recovery (mean± S.E.M) in Rate Pressure Product following ischaemia and reperfusion with or without pyruvate. * vs. pyruvate, $p<0.05$.

Kerr P et al. (1999). Am J Physiol 276, H496-H502

Modi P & Suleiman MS (2004). Amino Acids 26:65-70.

This work is supported by the British Heart Foundation.

Where applicable, the experiments described here conform with Physiological Society ethical requirements.

PC21

The mitochondrial permeability transition pore inhibitor cyclosporin A protects the immature heart against ischaemia and reperfusion injury

I.H. Khan[1], A.P. Halestrap[2], G.D. Angelini[1] and M. Suleiman[1]

[1]Bristol Heart Institute, University of Bristol, Bristol, UK and [2]Department of Biochemistry, University of Bristol, Bristol, UK

Cyclosporin A (CsA) inhibits opening of the mitochondrial permeability transition pore (MPTP), a critical event in some forms of myocardial necrotic and apoptotic cell death, by binding to cyclophilin D and inhibiting its peptidyl-prolyl cis-trans isomerase activity (Halestrap et al. 2004). Unlike in adult heart, little is known about the MPTP activity and role in immature heart. In this study we investigated the effect of CsA on recovery following ischaemia and reperfusion in isolated perfused immature heart.

Male Wistar rats (14 days old) were humanely killed, and the hearts were quickly removed, cannulated in the Langendorff mode and perfused with Krebs buffer at 37ºC as described previously (Modi & Suleiman 2004). After 20 min equilibration, hearts were exposed to normothermic global ischaemia for 60 minutes. Hearts were then reperfused for 50 min and functional recovery determined. In the experimental group 0.2 µmol/l CsA was present 10 min before and during ischaemia, but was washed out after 20 min reperfusion. Left ventricular developed pressure (and computed heart rate) was measured using a balloon inserted in the left ventricle. All results are expressed means ± S.E.M. and analysed using ANOVA with Fischer's PLSD post hoc test.

During pre-ischaemic perfusion, CsA had no effect on heart rate or LVDP. Time to induce contractile arrest was similar for both groups (5.3 ± 0.2 vs. 4.4 ±0.5min for CsA and control, respectively). The time to onset of ischaemic contracture was also similar (10.1 ± 1.0 vs. 7.8 ± 1.1min). Upon reperfusion, CsA significantly improved % recovery in rate pressure product (mmHg. beats min^{-1}) from 21% for control to 89%. Figure 1 shows time dependent change in LVDP in both groups.

This work shows that the MPTP inhibitor CsA is cardioprotective when added to immature heart during ischaemia and reperfusion. The protection is likely to be associated with changes in mitochondria upon reperfusion rather than during ischaemic arrest.

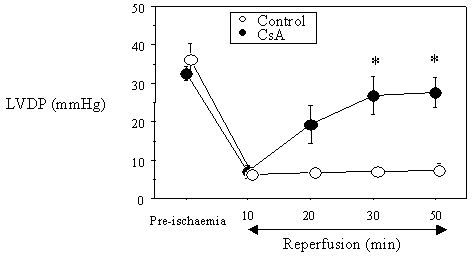

Figure 1. Changes in LVDP (mean± S.E.M) in immature rat hearts exposed to ischaemia and reperfusion with (n=4) or without (n=5) CsA. * vs. corresponding control, $p<0.05$.

Halestrap AP et al. (2004). Cardiovasc Res 61, 372-385.

Modi P & Suleiman MS (2004). Amino Acids 26, 65-70.

This work is supported by the British Heart Foundation.

Where applicable, the experiments described here conform with Physiological Society ethical requirements.

PC22

Neuropeptide Y and its receptor Y1 in diabetic rat heart

M. Chottova Dvorakova and J. Slavikova

Department of Physiology, Medical Faculty in Pilsen, Charles University, Pilsen, Czech Republic

Neuropeptide Y (NPY) is a 36-residue peptide amide produced by cleavage from a large precursor, preproNPY, that is widely dis-

tributed in the central and peripheral nervous system. In the periphery, NPY is co-stored and co-released with noradrenaline in sympathetic nerve fibres. Its actions are mediated through G protein-coupled receptors denoted Y1-Y6. In the rat heart, NPY mRNA is expressed in the cell bodies of intrinsic neurons and endothelial cells. The actions of NPY in the heart are extensive and include practically every cardiac cell type. The Y1 receptor induces vasoconstriction and regulates protein turnover and constitutive gene expression in hypertrophying cardiomyocytes. Investigations to date have implicated the role of NPY in the pathology of a number of diseases including diabetes (Pons et al. 2004).

Here, we investigated the involvement of this system in the events underlying development of diabetic cardiomyopathy in the rat model of streptozotocin (STZ)-induced diabetes by real-time RT-PCR, and immunohistochemistry. Wistar rats were humanely killed 6 and 9 months after intravenous application of STZ (65 mg/kg body weight). The quantitative RT-PCR reactions were carried out in a iCycler (BioRad). Relative gene expression was expressed as a ratio of target gene concentration to housekeeping gene. Statistical analysis of relative gene expression was done by Kruskal-Wallis test followed by Mann-Whitney test. Throughout, the results were considered significantly different when $p<0.05$. Expression of preproNPY mRNA was significantly lower in the left atrium 6 months after induction of the diabetes (n=5; mean=0.42; p=0.008), and it returns to control or slightly elevated levels 9 month of the duration of the disease (n=5; mean=1.39). The difference between STZ and vehicle-treated animals was not statistically significant. These changes were accompanied by initial up-regulation of Y1 receptor mRNA level at 6 month after application of STZ; however, statistical significance was not reached (n=5; p=0.16). Indirect immunofluorescence show NPY-immunoreactive (IR) nerve fibres distributed in myocardium and in the vicinity of coronary vessels in animals treated with vehicle. Some of these fibres displayed simultaneously dopamine beta-hydroxylase (DBH) immunolabelling indicating their sympathetic origin. In the hearts of animals both 6 and 9 months after STZ application, there were very few NPY-IR nerve fibres. Most of the fibres labelled by DBH antibody did not show NPY-IR. The persistence of Y1 receptors might contribute to the putative cardioprotective role of the NPY signalling system.

Pons J, Lee EW, Li L & Kitlinska J (2004). Curr Opin Investig Drugs 5, 957-962.

Supported by GACR 305/03/D180 and GACR 305/04/0144.

Where applicable, the experiments described here conform with Physiological Society ethical requirements.

PC23

Effect of age and hypertrophy on the contribution of the sarcoplasmic reticulum and sodium/calcium exchange to Ca^{2+} regulation in rat left ventricle

M.R. Fowler[1], J.R. Naz[1], M.D. Graham[1], G. Bru-Mercier[1], C.H. Orchard[2] and S.M. Harrison[1]

[1]Biomedical Sciences, University of Leeds, Leeds, West Yorkshire, UK and [2]Department of Physiology, University of Bristol, Bristol, UK

Compensated cardiac hypertrophy is associated with alterations in excitation-contraction (E-C) coupling. The resulting phenotype often includes enhanced Ca^{2+} transients and contraction. The present study investigated the progression of compensated hypertrophy by examining changes in Ca^{2+} flux pathways in 20 and 32 week (5 and 8 month) spontaneously hypertensive (SHR) and normotensive (WKY) rats.

Rats were humanely killed and left ventricular myocytes were isolated using a standard enzymatic dispersion technique and loaded with fura-2 to monitor intracellular Ca^{2+}. Cells were superfused with a physiological salt solution and Ca^{2+} transients elicited by field stimulation at 1 Hz. Data are presented as mean ± SEM and were analysed using two-way ANOVA, with significance assumed at 5%. Cell morphology was consistent with cellular hypertrophy in the SHR at 5 and 8 months of age (Table 1). Following steady-state stimulation, the Ca^{2+} content of the sarcoplasmic reticulum (SR) was assessed from the amplitude of the Ca^{2+} transient evoked by rapid application of 20 mM caffeine; Ca^{2+} transient amplitude and SR Ca^{2+} content were not significantly different in SHR myocytes at 5 and 8 months. The rate constant of decay (k) of the caffeine-evoked Ca^{2+} transient was examined in the absence and presence of Ni^{2+} to inhibit sodium calcium exchange (NCX). The component of Ca^{2+} decline attributable to SR Ca^{2+} uptake (i.e. k of the caffeine-evoked transient - k of the electrically-evoked Ca^{2+} transient) was not significantly affected by either strain or age. The Ni^{2+}-sensitive rate constant was also unaffected by strain, but was significantly increased by age (5 vs. 8 months (k, s^{-1}) WKY: 0.13 ± 0.01 vs. 0.22 ± 0.02, n=16/28, $P<0.05$. SHR: 0.11 ± 0.02 vs. 0.19 ± 0.02, n=18/18, $P<0.05$).

Calculation of relative activities from these rate constants showed a significant increase in the proportion of Ca^{2+} flux that occurred via NCX in the older animals, and an associated decrease in the proportion of Ca^{2+} taken up by the SR during the decay of the Ca^{2+} transient ($P<0.05$); these changes appear to be unaffected by hypertrophy.

	WKY 5 months	8 months	SHR 5 months	8 months
Cell length (μm)	133 Â± 3.3 (n=49)	138 Â± 5 (n=16)	127.5 Â± 2.5 (n=61)	129 Â± 5 (n=27)
Cell width (μm)	32.4 Â± 1	30.2 Â± 1.5	36.8 Â± 1*	40.2 Â± 2*
Cell volume (pL)	28.7 Â± 2	25.7 Â± 3.3	35 Â± 2*	41.4 Â± 4*
L:W ratio	4.2 Â± 0.2	4.7 Â± 0.3	3.6 Â± 0.14*	3.4 Â± 0.3*

Table 1. Cell dimensions in 5 and 8 month old SHR and WKY rats. *P<0.05 vs WKY at same age.

This work was supported by the British Heart Foundation.

Where applicable, the experiments described here conform with Physiological Society ethical requirements.

PC24

Mechanism of inhibition of the human ether-a-go-go related gene (HERG) potassium channel by the antipsychotic thioridazine

J.T. Milnes[1], H.J. Witchel[1], D.J. Leishman[2] and J.C. Hancox[1]

[1]Dept of Physiology, University of Bristol, Bristol, UK and [2]Ion Channel Pharmacology Group, Pfizer Global Research and Development, Sandwich, UK

The clinical use of the antipsychotic drug thioridazine (THIO) is associated with a significant risk of prolongation of the rate-

corrected QT interval of the ECG (Reilly et al. 2000). Most QT-prolonging drugs are associated with pharmacological blockade of the cardiac 'rapid' delayed rectifier K^+ current (I_{Kr}) and the current (I_{HERG}) carried by its cloned equivalent, HERG. THIO has been identified as an I_{Kr}/HERG blocker (Drolet et al. 1999). The aim of this study was to investigate the mechanism of I_{HERG} blockade by THIO.

Whole-cell patch-clamp experiments were performed at 37°C on Human Embryonic Kidney (HEK293) cells expressing either wild-type (WT) HERG or one of two S6-pore HERG-mutants:Y652A or F656A (these residues have been shown to be critical molecular determinants of HERG block by a number drugs). Cells were superfused with a physiological (Na^+-based) Tyrode's solution, and the pipette solution was a K^+-based intracellular salt solution.

THIO blocked WT-HERG IHERG with an IC_{50} of 91 nM (95% CI. 64.9-129.2 nM, 4 concentrations between 10nM and 5μM tested; n=4-5 at each) and Hill slope = 0.74 ± 0.04. Following equilibration in THIO (at either 0.1 or 1μM) block of I_{HERG} developed rapidly following onset of a sustained depolarization from -80mV to 0mV, consistent with an activation-dependent mechanism. The HERG S6 mutation Y652A partially attenuated HERG block by 1μM THIO, from 87 ± 1% (n=5) in WT-HERG to 55 ± 1% (n=5; t-test $p<0.05$). The S6 mutation F656A was highly resistant to 1μM THIO (a blockade of only 3 ± 5% was observed; n=5).

Collectively, these data are consistent with THIO being a high potency, open-channel HERG blocker binding within the channel pore cavity and with F656 being a critical determinant of drug binding and Y652 also having some influence.

Drolet et al, J Pharmacol Exp Ther. 1999; 288(3):1261-1268

Reilly et al. Lancet. 2000; 355:1048-1052

Where applicable, the experiments described here conform with Physiological Society ethical requirements.

PC25

The impact of voltage-clamp protocol on the apparent potency of a rapidly acting human ether-a-go-go related gene (hERG) potassium channel blocker

A. Alexandrou[1], J.T. Milnes[2], J.L. Leaney[1], J.C. Hancox[2] and D.J. Leishman[1]

[1]Pfizer Global Research and Development, Sandwich, UK and [2]Department of Physiology and Cardiovascular Research Labs, School of Medical Sciences, University of Bristol, Bristol, UK

Drug-induced QT interval prolongation can lead to the potentially life threatening arrhythmia Torsade de Pointes and is believed to result primarily from inhibition of the hERG-mediated potassium (K^+) current in the heart. Prolongation of the QT interval of the electrocardiogram has now been observed for a number of compounds including both antiarrhythmic agents and non-cardiovascular related drugs (Pourrias et al. 1999). Therefore, an important aspect of safety pharmacology is to determine the potency of new drugs in blocking hERG channels and understand their mechanism of block.

External and in-house studies have shown that certain compounds investigated seem to exhibit distinct profiles of hERG channel block. The objectives of this study were to examine the inhibition of hERG K^+currents (I_{hERG}) by the novel hERG blocker, CONA-437 ([4-(3-methoxy-4-methylsulfanyl-phenoxy)-pyridin-3-ylmethyl]-dimethyl-amine), using different voltage clamp protocols and to characterize the nature of block for this type of compound.

A human embryonic kidney (HEK293) cell line stably expressing the hERG K^+ channel (Zhou et al. 1998) was used to study I_{hERG} at 37°C using the whole-cell patch-clamp technique. Cells were superfused with a physiological Na^+-based extracellular solution and patch pipettes were filled with a K^+-based intracellular solution supplemented with MgATP. Data were acquired and analysed using Axon Instruments pClamp suite of software.

We have used a number of different voltage protocols in order to evoke I_{hERG}: a step-ramp command (at room temperature and 37°C) (hold −80mV, step +20mV for 1s, ramp to−80mV at 0.5mV/ms), a physiological ventricular action potential command and a 2-step protocol (hold−80mV, step +20mV for 2s, step−40mV). These yielded IC_{50} values of 987nM (95% CI: 0.78—1.24μM), 1.34μM (95% CI: 0.98—1.83μM), 717nM (95% CI: 610—843nM) and 2.42μM (95% CI: 1.97—2.97μM) respectively.

Apparent potency of I_{hERG} block by CONA-437 does not seem to vary markedly with voltage protocol or temperature. However, development of block with this compound also appears rapid. Envelope-of-tails and sustained depolarisation (−80 mV to 0 for 10 s) voltage protocols revealed that onset of I_{hERG} blockade was extremely rapid and occurred within 200ms.

Zhou Z et al. (1998). Biophysical Journal 74, 230-241.

Pourrias B et al (1999). Drug Development Research 47, 55-62.

Where applicable, the experiments described here conform with Physiological Society ethical requirements.

PC26

Evidence against gating-independent inhibition of the HERG potassium channel by ketoconazole

J.M. Ridley, J.T. Milnes, H.J. Witchel, R.S. Duncan and J.C. Hancox

Physiology, University of Bristol, Bristol, UK

Pharmacological inhibition of HERG (*human ether-a-go-go-related gene*) potassium channels by therapeutically diverse drugs is considered to involve a binding site within the inner cavity, involving aromatic amino-acids in the channel inner (S6) helix which are rendered accessible on channel gating (Mitcheson & Perry, 2003). However, the antimycotic drug ketoconazole has been suggested previously to inhibit HERG channel current (I_{HERG}) without a requirement for channel activation, based on observations made using the *Xenopus* oocyte expression system (Dumaine et al. 1998). The aim of the present study was to determine whether or not ketoconazole inhibits I_{HERG} from a mammalian (Human Embryonic Kidney, HEK293) cell line, independently of channel gating.

Whole-cell patch-clamp measurements of I_{HERG} were made at 37°C using HERG stably expressed in HEK293 cells. Five dif-

ferent concentrations of ketoconazole ranging from 50 nM to 50 μM were applied (n = at least 5 cells per concentration) and inhibition of I_{HERG} tails at -40 mV (following a 2 s activating pulse from -80 mV to +20 mV) was monitored. Ketoconazole inhibited I_{HERG} tails with a half-maximal inhibitory concentration (IC_{50}) of 1.8 μM (C.I. 965.0 nM to 3.4 μM). The profile of I_{HERG} blockade during a 12 s ascending voltage ramp between -80 and +40 mV (n = 5 cells) was inconsistent with a predominantly closed-state channel blocking effect and blockade was also observed to be time-dependent during application of a sustained depolarisation from -80 to 0 mV (n = 6 cells). Importantly, the S6 mutant F656A (phenylalanine to alanine) significantly attenuated the inhibitory effect of ketoconazole (20 μM ketoconazole inhibited WT-HERG by 88.6 ± 1.7%; mean ± S.E.M.; n = 5 and F656A-HERG by 24.9 ± 3.4 %; n = 5 $p < 0.001$; unpaired Student's t test). These observations provide evidence that ketoconazole inhibits I_{HERG} by gaining access to its binding site on channel gating; thus is inconsistent with a major role for closed-state channel inhibition by this agent.

Dumaine R *et al* (1998). *J Pharmacol Exp Ther* **286**, 72.

Mitcheson JS & Perry MD (2003). *Curr Opin Drug Discov Devel.* **6**, 667-674.

Where applicable, the experiments described here conform with Physiological Society ethical requirements.

PC27

Phosphorylation of the sheep cardiac ryanodine receptor modifies both gating and conductance

S. Carter[1], J. Colyer[2] and R. Sitsapesan[1]

[1]Dept. of Pharmacology, University of Bristol, Bristol, UK and [2]Biochemistry and Molecular Biology, University of Leeds, Leeds, UK

Protein kinase A (PKA)-dependent phosphorylation of the cardiac ryanodine receptor (RyR) is a controversial subject; some groups report an increase in single-channel open probability (P_o) (1), while others report a reduction in P_o and [^{3}H]ryanodine binding (2). We have therefore investigated how the degree of phosphorylation at serine 2809 (S2809) is related to the single-channel function of the sheep cardiac RyR.

Sarcoplasmic reticulum membrane vesicles were isolated (4) from sheep hearts obtained from an abattoir and were either incorporated into artificial membranes for single-channel studies or were used for [^{3}H]ryanodine binding or Western blotting. All data presented, unless stated otherwise, are mean ± SEM, and statistical significance was determined using a paired t test ($n \geq 4$). Cardiac RyR channels were found to exhibit a relatively high level of basal phosphorylation at S2809 (76.5 ± 9.8 % of maximum (SD; n=3)) that was associated with relatively low P_o under various conditions (0.050 ± 0.019 in the presence of 10 μM Ca^{2+}). Despite this high level of phosphorylation, addition of the catalytic subunit of PKA to the cytosolic channel face, in the presence of ATP and Mg^{2+}, resulted in a significant increase in P_o that was maintained after PKA was removed (0.145 ± 0.077 to 0.643 ± 0.197 ($p<0.05$) in the presence of 10 μM Ca^{2+}, 10 mM ATP, and 0.5 mM Mg^{2+}). The increase in P_o was also associated with a significant increase in single-channel current amplitude at a holding potential of 0 mV (4.12 ± 0.09 to 4.53 ± 0.05 pA and 3.69 ± 0.16 to 4.12 ± 0.16 pA ($p>0.01$) in the presence of 50 μM Ca^{2+} and 10 μM Ca^{2+}, 10 mM ATP, and 0.5 mM Mg^{2+} respectively). In contrast, maximum PKA-dependent phosphorylation at S2809, as demonstrated by phosphorylation state specific antibodies (3), led to a significant reduction in [^{3}H]ryanodine binding to 78.1 ± 2.1%, 77.7 ± 0.4%, and 29.8 ± 5.7% ($p<0.01$) of control binding at free [Ca^{2+}] of 50 μM, 10 μM, and 1 μM.

Our results indicate that increases in the level of phosphorylation at S2809 produce little change in channel function until very high or maximum levels of phosphorylation are reached, at which point, maintained high P_o values and increased conductance are achieved. Since our [^{3}H]ryanodine binding studies suggest that phosphorylation of S2809 leads to a decrease in P_o, we conclude that the overall effect of phosphorylation at S2809 may depend on a complex combination of factors influencing channel gating including the presence of other associated proteins.

Marx SO et al. (2000). Cell 101, 365-376.

Valdivia HH et al. (1995). Science 267, 1997-2000.

Rodriguez P et al. (2003). J Biol Chem 278, 38593-38600.

Kermode H et al. (1998). FEBS Lett 431, 59-62.

This work was supported by the British Heart Foundation.

Where applicable, the experiments described here conform with Physiological Society ethical requirements.

PC28

The effect of different fixation protocols on immunocytochemical labelling of ion channels in rat ventricular myocytes

T.T. Yamanushi[1], M.R. Boyett[2] and H. Dobrzynski[2]

[1]Kagawa Prefectural College of Health Sciences, Kagawa, Japan and [2]Cardiovascular and Endocrine Sciences, University of Manchester, Manchester, UK

Immunocytochemistry is an established method to identify the localization of cellular proteins. The aim of the present study was to investigate the effect of different fixation treatments on immunocytochemical labelling of ion channels in enzymatically isolated rat ventricular myocytes from humanely killed rats. Two different fixation protocols were employed. In the first fixation protocol, cells were fixed in paraformaldehyde (PFA, 4%) for 30 min at room temperature and incubated with 0.1% Triton X-100 in PBS (which permeabilizes surface membranes as well as those of intracellular organelles). With the second fixation protocol, fixation and permeabilization was performed by incubating cells with ice-cold 100% methanol (MeOH) for 5 min at -20°C. After PFA or MeOH fixation all cells were subjected to the same protocol. They were washed in PBS and blocked with 10% donkey serum in PBS. Following 14-22 h incubation with primary antibodies at 4°C, cells were washed in PBS, incubated

with secondary antibodies conjugated to FITC and visualized using laser scanning confocal microscopy. With these two fixation protocols, labelling of various ion channels was investigated: $K_v1.5$ (responsible for I_{Kur}, Fig. 1), $K_v4.2$ (responsible for I_{to}), $K_v7.1$ (K_vLQT1, responsible for I_{Ks}), $K_v11.1$ (ERG, responsible for I_{Kr}), $K_{ir}2.2$ (responsible for I_{K1}), $K_{ir}6.2$ (responsible for I_{KATP}), $Ca_v1.2$ (α_{1C}, responsible for I_{CaL}), $Ca_v1.3$ (α_{1D}, responsible for I_{CaL}), $Ca_v\alpha_1$ (α_{1C} and α_{1D}) and $Ca_v3.1$ (α_{1G}, responsible for I_{CaT}). With PFA fixation, there was a distinct and strong striated pattern of labelling (presumably corresponding to t-tubules) of $K_v4.2$, $K_{ir}6.2$ and $Ca_v\alpha_1$ and a weak striated pattern of labelling of $K_v1.5$ (Fig. 1), but no labelling of other ion channels. With MeOH fixation, there was a distinct and strong striated pattern of labelling of $Ca_v1.2$, $Ca_v1.3$ and $Ca_v\alpha_1$, a weak striated pattern of labelling of $K_v1.5$ and labelling at intercalated discs in the case of $K_v1.5$ (Fig. 1), $Ca_v\alpha_1$ and $Ca_v3.1$, but no labelling of other ion channels. Results are summarised in Table 1. This study clearly demonstrates the importance of different fixation protocols on the labelling of ion channel proteins in myocytes. It is concluded that, to visualise ion channels in the heart using immunolabelling, the results obtained from both PFA and MeOH fixation protocols should be compared.

Table 1. Effect of two different fixation protocols on immunolabelling of ion channels

Channel	PFA fixation	MeOH fixation
$K_v1.5$	+ (t-tubules)	+ (t-tubules, intercalated discs)
$K_v4.2$	+ (t-tubules)	-
$K_v7.1$	-	-
$K_v11.1$	-	-
$K_{ir}2.2$	-	-
$K_{ir}6.2$	+ (t-tubules)	-
$Ca_v1.2$	-	+ (t-tubules)
$Ca_v1.3$	-	+ (t-tubules)
$Ca_v\alpha_1$	+ (t-tubules)	+ (t-tubules, intercalated discs)
$Ca_v3.1$	-	+ (intercalated discs)

The presence (+) or absence (-) of labelling and the site of labelling, if present, is noted. For each fixation protocol and channel studied, immunolabelling was imaged in three cells (except in cases in which there was no labelling); in all cases, the pattern of labelling in the cells imaged was typical.

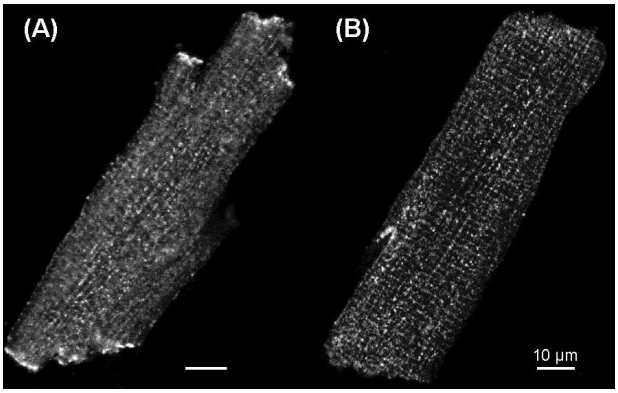

Figure 1. The effect of two different fixation treatments on immunolabelling of $K_v1.5$. A, strong labelling at intercalated discs (e.g. at arrow) with MeOH fixation. B, weak striated pattern of labelling with PFA fixation. Using a different $K_v1.5$ antibody and MeOH fixation, strong labelling of $K_v1.5$ at the intercalated disc was previously observed in rat ventricular myocytes (Dobrzynski et al. 2000).

Dobrzynski et al. (2000). J Histochem Cytochem 48, 769-780.

Where applicable, the experiments described here conform with Physiological Society ethical requirements.

PC29

Cardiac and neuronal sodium currents are differentially localized in rat ventricular myocytes

F. Brette[1], Y. Korchev[2] and C.H. Orchard[1]

[1]Department of Physiology, University of Bristol, Bristol, UK and [2]MRC Clinical Sciences Centre, Imperial College, London, UK

Immunocytochemistry data suggest that neuronal Na channels are present at the transverse (t-) tubules of cardiac ventricular myocytes (Maier *et al.* 2002); however, no data about the distribution of function (i.e. current) are available. In the present study, we recorded Na current (I_{Na}) in control and detubulated myocytes (Brette *et al.* 2002), which enabled us to determine and quantify the functional localization of specific isoforms of I_{Na} in rat ventricular myocytes. Wistar rats were killed humanely. Ventricular myocytes were enzymatically isolated, and detubulated using formamide as described by Kawai *et al.* (1999). The whole-cell configuration of the patch clamp technique was used to record I_{Na}. To ensure good voltage control, extracellular [Na] was decreased to 20 mM, low resistance pipettes were used (1.5 ± 0.1 MΩ, mean ± S.E.M., n=32) and series resistance (2.8 ± 1.1 MΩ, n=32) was compensated by 85-90%. I_{Na} was elicited by a test pulse to −40 mV from a holding potential of −120 mV. Neuronal I_{Na} was assessed as the current sensitive to a low (100 nM) concentration of TTX (Maier *et al.* 2002). Experiments were performed at room temperature (22-24°C).

Cell capacitance was significantly smaller in detubulated cells than in control cells (in pF: 137 ± 7 vs 199 ± 9, n=15 and 17, respectively, $P<0.05$, two tailed unpaired t test); however, I_{Na} density (in pA/pF: 73 ± 5 (control) vs 81 ± 8 (detubulated), NS) and time to peak (in ms: 1.39 ± 0.08 (control) vs 1.42 ± 0.07 (detubulated) NS) were unchanged. 100 nM TTX blocked 24 ± 2% of I_{Na} in control myocytes and 8 ± 2% in detubulated myocytes, suggesting that more neuronal I_{Na} (I_{NaN}) is present in control, than in detubulated myocytes ($P<0.05$, unpaired t-test). From these data, we calculated the relative distribution of currents as previously described (Despa et al. 2003). The cardiac I_{Na} (I_{NaC}, residual I_{Na} during application of 100 nM TTX) appears to be almost exclusively present at the surface membrane (95%) where it is 10 times more concentrated than in the t-tubules. In contrast, I_{NaN} is located predominantly in the t-tubules (75%) where it is 6.4 times more concentrated than at the surface membrane. We conclude that although I_{Na} is uniformly distributed between the t-tubules and surface membrane of rat ventricular myocytes, this masks a marked differential localization of I_{Na} isoforms, which suggests specific physiological roles for I_{NaC} (e.g. excitability & conduction) and I_{NaN} (e.g. t-tubule excitability).

Brette F *et al.* (2002). Am J Physiol 283, 1720-8.

Despa *et al.* (2003). Biophys J 85, 3388-96.

Kawai M *et al.* (1999). Am J Physiol 277, H603-609.

Maier SK *et al.* (2002). PNAS 99, 4073-8.

Supported by the Wellcome Trust.

Where applicable, the experiments described here conform with Physiological Society ethical requirements.

PC30

Molecular mapping of the rabbit sinoatrial node

J. Tellez[1], H. Dobrzynski[1], I.D. Greener[2], G.M. Graham[2], H. Honjo[3], M. Yamamoto[3], M.R. Boyett[1] and R. Billeter[2]

[1]University of Manchester, Manchester, UK, [2]University of Leeds, Leeds, UK and [3]Nagoya University, Nagoya, Japan

The sinoatrial node (SAN) is the pacemaker of the heart. Although the ionic currents responsible for pacemaker activity have been recorded from rabbit SAN, little is known about the molecular basis of these ionic currents. The aim of our study was to measure levels of mRNA coding for specific ion channels and their associated subunits in the rabbit SAN and surrounding atrial tissue.

Rabbits were killed humanely and the SAN isolated. For quantitative PCR, cDNA was synthesised from tissue dissected from the centre and periphery of the SAN, as well as from the right atrium (RA; n=7 rabbits). All PCRs were performed in triplicate. Table 1 summarises the transcripts for which cDNA levels were significantly different between tissue samples. No significant differences in mRNA levels were found for Kv4.3, KChIP2, Kir2.1, Kir2.2, Kir3.1, Cx45, NCX1, SERCA2a, 28S and GAPDH. *In situ* hybridisation was performed with probes targeted to specific transcripts. The localisation of the *in situ* hybridisation labelling was in the main consistent with the quantitative PCR data.

These results show that mRNA levels for ion channels and associated regulatory subunits vary within the rabbit SA node and between the SA node and surrounding atrial tissue. The pattern of expression of ion channels helps explain the ionic currents recorded.

Table 1. Number of cDNA molecules relative to number of cDNA molecules in RA (100 %)

Target	SAN periphery (%)	SAN centre (%)
ANP	12 ± 3*	6 ± 2*
NFM	4793 ± 1292*	5294 ± 1509*
HCN1	118 ± 11	332 ± 133*#
HCN4	888 ± 358*	1986 ± 943*#
$Ca_v1.2$	50 ± 7*	64 ± 27*
$Ca_v1.3$	403 ± 47*	6038 ± 110*#
RYR2	40 ± 7*	45 ± 12*
$Na_v1.1$	383 ± 92*	305 ± 84*
$Na_v1.5$	32 ± 11*	17 ± 4*
Kv1.4	18 ± 5*	29 ± 10*
Kv1.5	172 ± 51	47 ± 21*#
Kv4.2	214 ± 52*	364 ± 112*
ERG	126 ± 16	171 ± 47*
KvLQT1	126 ± 9	148 ± 23*
Kir6.2	44 ± 9*	28 ± 4*
SUR2A	55 ± 8*	42 ± 9*
Cx40	68 ± 13	54 ± 12*
Cx43	38 ± 7*	26 ± 11*

*Significant difference compared to RA (P<0.05), #significant difference compared to SAN periphery (P<0.05). Significance of differences was calculated using one-way ANVOA. Data are shown as means ± S.E.M.

Where applicable, the experiments described here conform with Physiological Society ethical requirements.

PC31

Charged residues on the S5-P extracellular linker modulate inactivation characteristics of EAG family K^+ channels

C.E. Clarke and J.I. Vandenberg

Electrophysiology and Biophysics, St Vincent's Clinical Medical School, UNSW and Victor Chang Cardiac Research Institute, Sydney, NSW, Australia

The human ether-a-go-go related gene (HERG) has unusual kinetics with slow activation but very rapid and voltage-dependent inactivation. HERG inactivation is affected by mutations in the outer mouth region of the channel. The outer pore region of HERG K^+ channels has a much longer S5-P linker than other voltage-gated K^+ channels and contains an amphipathic α-helix that modulates inactivation (Liu et al. 2002; Torres et al. 2003). The rat EAG-like (ELK) channel (RELK2) possesses a similarly long S5-P linker but has markedly reduced C-type like inactivation in comparison to HERG channels. To investigate the molecular basis of these differences we made chimaeras between HERG and RELK2 and studied their inactivation properties in *Xenopus* oocytes using standard inactivation protocols (Torres et al. 2003). All data are mean ± S.E.M.

The $V_{0.5}$ of inactivation of RELK2 channels was 31.8 ± 3.4 mV (n=5) compared to $V_{0.5}$ of -70.3 ± 6.1 mV (n=6) for WT HERG. A chimaeric channel consisting of HERG but with the α-helix from the S5-P region of RELK2 (HERG/ELK S5P) had inactivation characteristics resembling WT RELK2 channels ($V_{0.5}$ of 27.3 ± 0.3 mV, n=4). This confirms the importance of this region in inactivation.

Whilst the structure of the amphipathic helix in the S5-P linker is predicted to be the same in the HERG/RELK2 S5-P chimaera as WT HERG and the hydrophobic residues in this segment are highly conserved, there are significant variations in the hydrophilic residues. N588 in HERG is replaced with a glutamate in RELK2 and D591 and Q592 are replaced with arginines. Mutation of HERG N588E resulted in channels that rapidly inactivated with a $V_{0.5}$ of inactivation of -109 ± 5.2 mV (n=5). The HERG D591R/Q592R double mutant displayed current characteristics similar to both WT RELK2 and the S5-P chimaera with a $V_{0.5}$ of inactivation of 28.7 ± 3.3 mV (n=5). Mutation of both HERG N588E and D591R/Q592R together led to a channel with functional characteristics similar to D591R/Q592R alone ($V_{0.5}$ of inactivation of 26.9 ± 1.7 mV (n=5)), highlighting the severity of inactivation disruption with the presence of positive charges on the S5-P loop. A simple model for the role of the S5-P in inactivation that is consistent with our data is that the S5-P amphipathic helix interacts with a positively charged region elsewhere on the channel. Consequently, the addition of negative charge (e.g. N588E) enhances inactivation, whereas the addition of positive charge (e.g. D591R/Q592R) inhibits inactivation.

Liu J et al. (2002). J Gen Physiol 120, 723-737.

Torres A et al. (2003). J Biol Chem 278, 42136-48.

Supported by the NHMRC. C.E.C. is an ARC Postdoctoral Fellow.

Where applicable, the experiments described here conform with Physiological Society ethical requirements.